Supplementary Information

Highly Specific Enrichment of Rare Nucleic Acid Fractions using *Thermus thermophilus* Argonaute with Applications in Cancer Diagnostics

Jinzhao Song[1,*,†], Jorrit W. Hegge[2,†], Michael G. Mauk[1], Junman Chen[1], Jacob E. Till[3], Neha Bhagwat[3], Lotte T. Azink[2], Jing Peng[1], Moen Sen[3], Jazmine Mays[3], Erica Carpenter[3], John van der Oost[2,*], and Haim H. Bau[1,*]

[1] Department of Mechanical Engineering and Applied Mechanics, University of Pennsylvania, Philadelphia PA, USA
[2] Laboratory of Microbiology, Department of Agrotechnology and Food Sciences, Wageningen University, The Netherlands
[3] Perelman School of Medicine, University of Pennsylvania, Philadelphia PA, USA

* To whom correspondence should be addressed. Tel: 2158981380; Fax: 215-573-6334; Email: songjinz@seas.upenn.edu, Correspondence may also be addressed to john.vanderoost@wur.nl, bau@seas.upenn.edu

[†]The authors wish it to be known that, in their opinion, the first 2 authors should be regarded as joint First Authors

S1: Buffer Optimization 2
S2: The effect of guide DNA mismatch position on cleaving efficiency 9
S3: The effects of guide length and temperature on *Tt*Ago cleavage 14
S4: *Tt*Ago cleavage of dsDNA 16
S5: CRISPR/Cas9-based dsDNA cleavage 21
S6: NAVIGATER improves the sensitivity of downstream rare allele detection 22
S7: Multiplexed enrichment 25
S8: Detection methods of low-frequency (<0.2%) cancer mutations in clinical cell-free DNA 29
S9: *Tt*Ago Purification 34
S10: Thermal deactivation of *Tt*Ago 35
Supplementary References 36
Supplementary Note 1: The sequences of guides and synthetic targets 37

Supplemental Section 1: Buffer Optimization

For rapid and inexpensive genotyping of rare mutant alleles, we envision using NAVIGATER in combination with enzymatic amplification of rare nucleic acids, in either a single-stage or a two-stage process. Isothermal amplification schemes such as Loop Mediated Isothermal Amplification (LAMP) (1) are of particular interest since they do not require temperature cycling and can be carried out with simple instrumentation in real time next to the patient or in resource-poor settings (2). Therefore, we tested *Tt*Ago's endonucleolytic activity in various LAMP buffers and in Buffer S (3) (Supplementary Table 1).

We incubated *Tt*Ago with either single-strand (ss) DNA or ssRNA fragments (100 nt) of the human *KRAS* gene and a 16 nt DNA oligo guide that complements the wild type (WT) *KRAS,* but has a single nucleotide mismatch at position 12 (g12) with *KRAS*-G12D. *Tt*Ago performed best in Buffer 3, exhibiting nearly 100% cleaving efficiency of complementary WT DNA and RNA and low cleaving efficiency (<1%) of mutant alleles (Supplementary Figs. 1a and 3a) at 80°C.

In contrast to our other buffers, Buffer 3 contains betaine, dNTPs, and a higher concentration of magnesium (8 mM vs 2 mM). To examine the effect of each of these components on *Tt*Ago's activity, we added each separately to Buffer 2 and Buffer S. Consistent with earlier studies (3-6), the presence of divalent cations, such as Mg^{2+}, improves *Tt*Ago's endonucleolytic activity. High concentrations of magnesium (≥8 mM) are essential for high level of activity at high temperatures (e.g., 80°C) (Supplementary Figs. 1 and 3).

Betaine significantly increases DNA cleavage efficiency (Supplemental Figs. 1b, c), but to a lesser degree RNA cleavage efficiency (Supplemental Fig. 3d). Supplementing Buffer 2 and Buffer S with both Mg^{2+} (6 mM) and betaine (0.8 M) increased *Tt*Ago cleavage efficiency from 60-80% to nearly 100% (Supplementary Figs. 1b, c). This is consistent with betaine ability to enhance thermal stability of polymerase enzymes (7) and to dissolve secondary GC structure(8).

Surprisingly, dNTPs caused the greatest increase in cleavage efficiency of RNA (Supplementary Figs. 3b, c, e, f). To verify that this beneficial effect is not unique to *KRAS*, we also tested dNTPs' effect on the cleavage efficiency of *EFGR* sequences (Supplementary Fig. 5). In the absence of dNTPs, the cleavage efficiency of *EGFR* WT RNA is 45% while in the presence of 1.4 mM dATP, dTTP or dCTP, it increased to nearly 100%. Addition of 1.4 mM dGTP did not affect cleavage efficiency. Among NTPs, only CTP increased the cleavage efficiency of WT RNA (Supplementary Fig. 5b). Although the molecular basis of this enhancement is still elusive, the combination of dNTPs' sugar groups and nitrogenous bases appears to stimulate *Tt*Ago's activity. *Tt*Ago is most active when buffer pH ranges from 8 to 9 (Supplementary Fig. 5c).

In summary, betaine, dNTPs, and Mg^{2+} enhance *Tt*Ago's activity without adversely affecting its single nucleotide specificity. Remarkably, the same buffer is suitable for cleaving both DNA and RNA. In the remainder of this paper, we use Buffer 3.

Supplementary Table 1. Buffer compositions

Buffer 1 ThermoPol® Reaction Buffer (1X, NEB)	**Buffer 2** Isothermal Amplification Buffer (1X, NEB)	**Buffer 3** Eiken buffer (1X)	**Buffer S**(3) Buffer of Swarts et.al.
20 mM Tris-HCl	20 mM Tris-HCl	20 mM Tris-HCl	10 mM Tris-HCl
10 mM $(NH_4)_2SO_4$	10 mM $(NH_4)_2SO_4$	10 mM $(NH_4)_2SO_4$	125 mM NaCl
10 mM KCl	50 mM KCl	10 mM KCl	2 mM $MgCl_2$
2 mM $MgSO_4$	2 mM $MgSO_4$	8 mM $MgSO_4$	(pH 8.0 at 25°C)
0.1% Triton X-100	0.1% Tween 20	0.1% Tween 20	
(pH 8.8 at 25°C)	(pH 8.8 at 25°C)	0.8 M Betaine	
		1.4 mM dNTPs	
		(pH 8.8 at 25°C)	

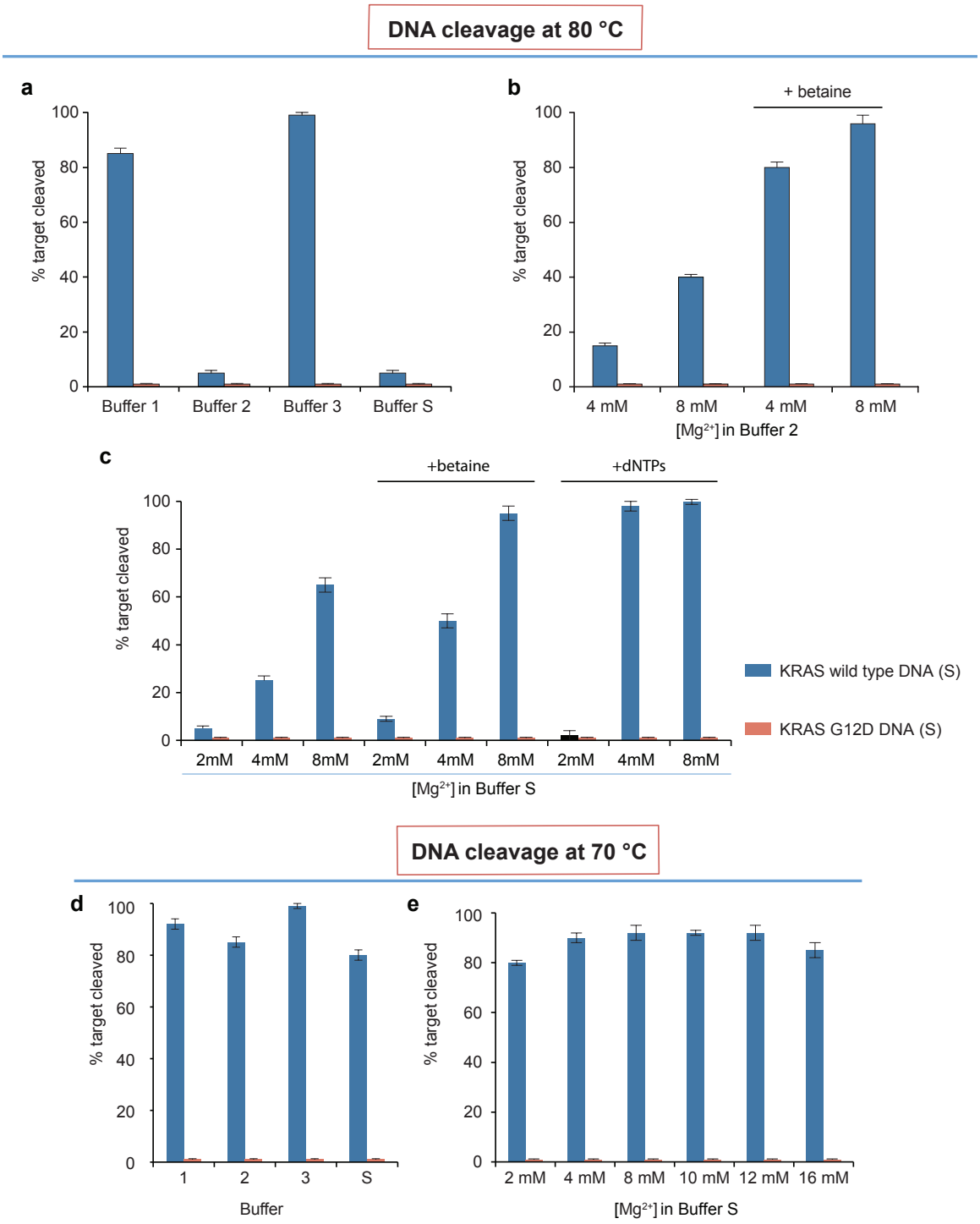

Supplementary Figure 1: Betaine, Mg^{2+}, and dNTPs enhance *Tt*Ago DNA cleavage. (**a**) DNA cleavage as a function of buffer composition (Supplementary Table 1) at 80°C. (**b**) DNA cleavage in Buffer 2 as a function of [Mg^{2+}] in the absence and presence of betaine at 80°C. (**c**) DNA cleavage in Buffer S as a function of [Mg^{2+}] in the absence and presence of betaine (0.8 M) or dNTPs (1.4 mM) at 80°C. (**d**) DNA cleavage as a function of buffer composition at 70°C. (**e**) DNA cleavage in Buffer S as a function of [Mg^{2+}] at 70°C. All experiments were carried out with *KRAS* Sense (S) strand and 16 nt *KRAS*-S MP12 guide. Incubation time 20 min. *Tt*Ago: guide: target =5: 1: 1 (1.25 µM : 0.25 µM : 0.25 µM). N=3.

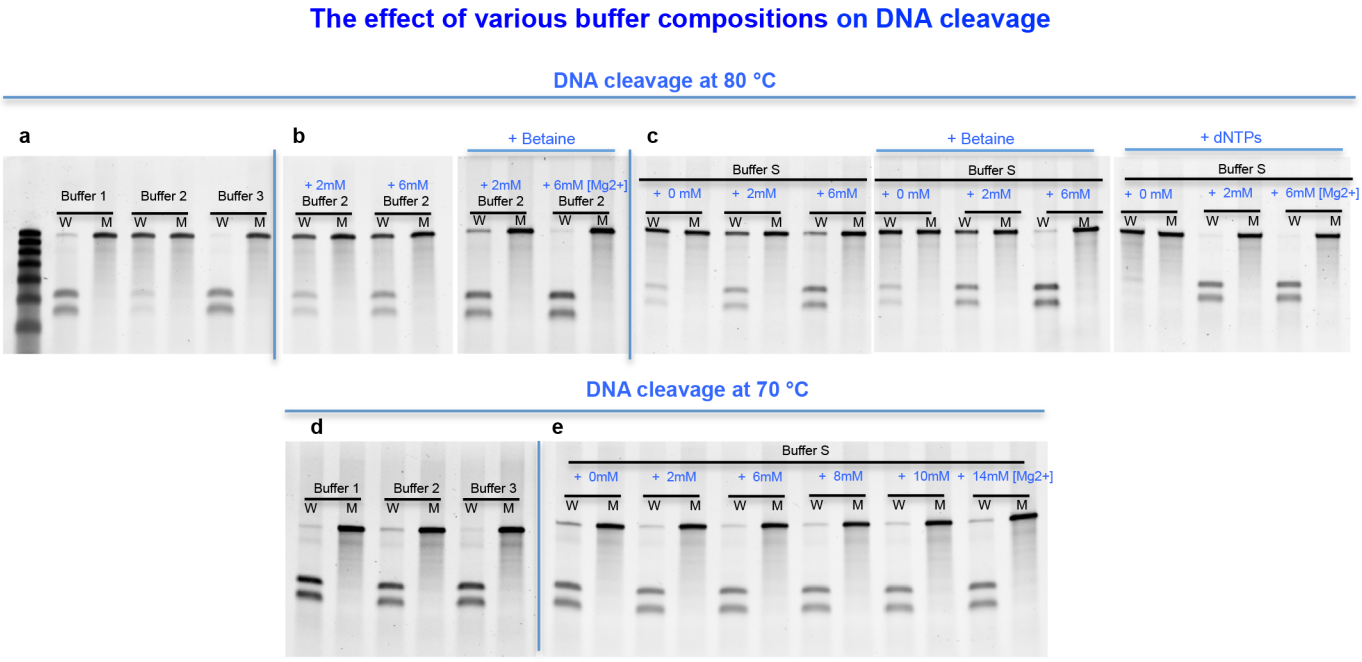

Supplementary Figure 2: **Electropherograms of *Tt*Ago cleavage products of WT *KRAS* (W) and *KRAS* G12D (M) sense ssDNA after 20 min incubation in Buffers 1, 2, 3, and S (Supplementary Table 1) in the presence and absence of additives.** (**a**) Buffers 1, 2, 3, and S. 80°C, no additives. (**b**) Buffer 2. Various [Mg^{2+}] in the absence and presence of betaine (0.8 M), 80°C. (**c**) Buffer S. Various [Mg^{2+}] in the absence and presence of betaine (0.8 M) or dNTPs (1.4 mM), 80°C. (**d**) Buffers 1, 2, 3. 70°C, no additives. (**e**) Buffer S. Various [Mg^{2+}], 70°C. *Tt*Ago: guide: target =5: 1: 1. N=3.

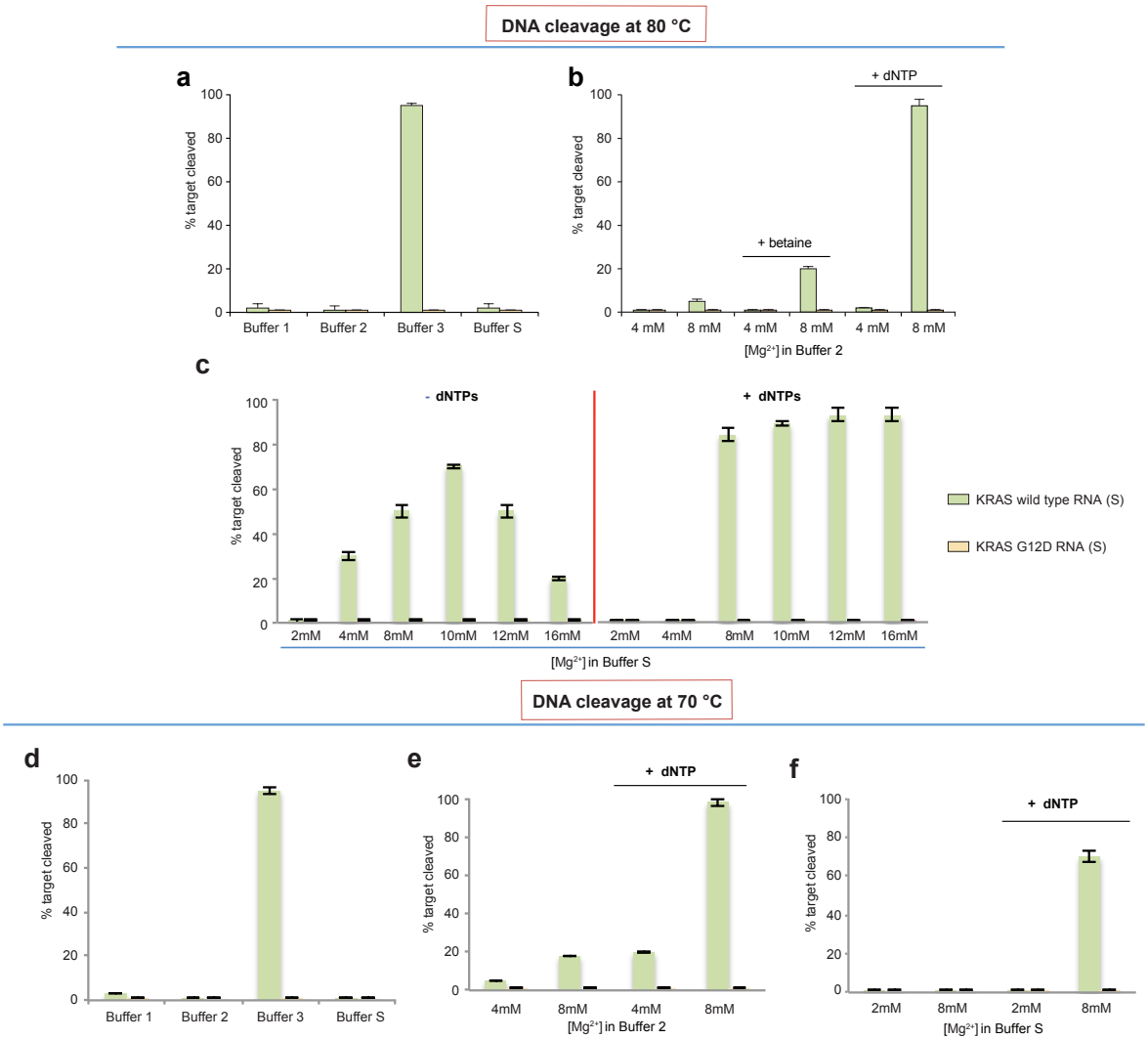

Supplementary Figure 3: Betaine, Mg^{2+}, and dNTPs enhance *Tt*Ago RNA cleavage. (**a**) RNA cleavage as a function of buffer composition (Supplementary Table 1) at 80°C. (**b**) RNA cleavage in Buffer 2 as a function of [Mg^{2+}] in the absence and presence of betaine (0.8 M) or dNTPs (1.4 mM) at 80°C. (**c**) RNA cleavage in Buffer S as a function of [Mg^{2+}] in the absence and presence of dNTPs (1.4 mM) at 80°C. (**d**) RNA cleavage as a function of buffer composition at 70°C. (**e**) RNA cleavage in Buffer 2 as a function of [Mg^{2+}] in the absence and presence of dNTPs (1.4 mM) at 70°C. (**f**) RNA cleavage in Buffer S as a function of [Mg^{2+}] in the absence and presence of dNTPs (1.4 mM) at 70°C. All experiments were carried out with *KRAS* Sense (S) strand and 16 nt *KRAS*-S MP12 guide. Incubation time 20 min. *Tt*Ago: guide: target =5: 1: 1 (1.25 µM : 0.25 µM : 0.25 µM). N=3.

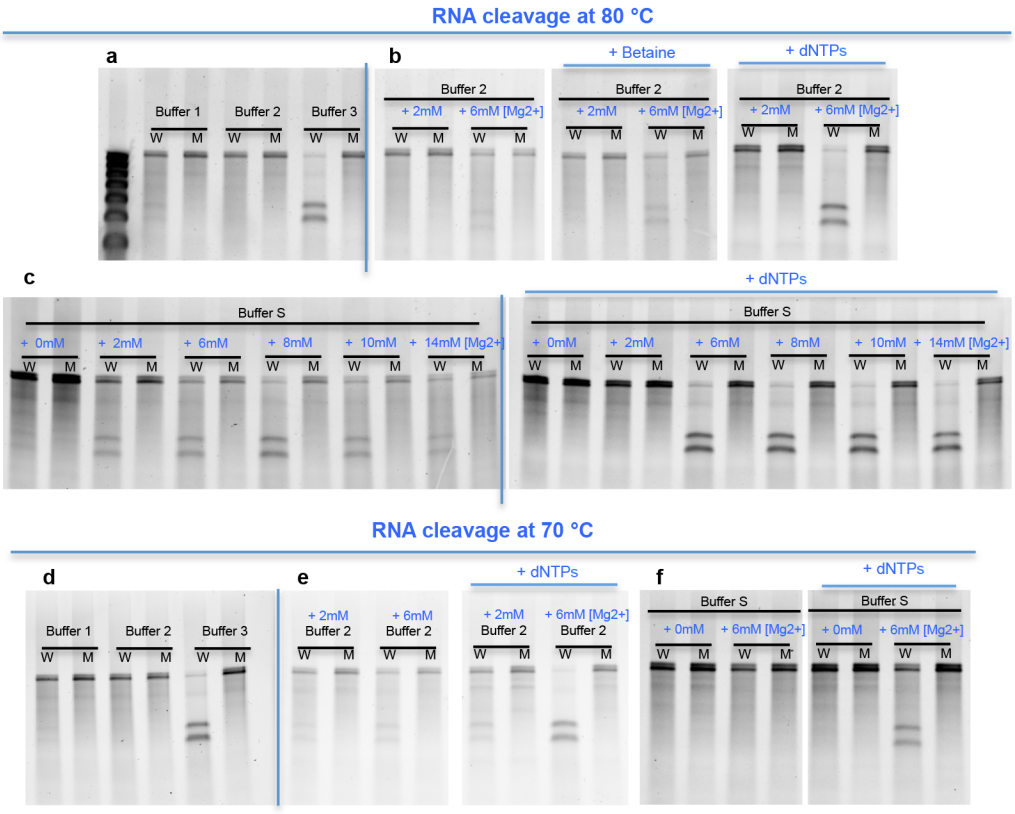

Supplementary Figure 4: **Electropherograms of *Tt*Ago cleavage products of WT *KRAS* (W) and *KRAS* G12D (M) RNA after 20 min incubation in Buffers 1, 2, 3, and S (Supplementary Table 1) in the presence and absence of additives.** (**a**) Buffers 1, 2, and 3. 80°C, No additives. (**b**) Buffer 2. Various [Mg^{2+}] in the absence and presence of betaine (0.8 M) or dNTPs (1.4mM), 80°C. (**c**) Buffer S. Various [Mg^{2+}] in the absence and presence of dNTPs (1.4 mM), 80°C. (**d**) Buffers 1, 2, and 3. 70°C, No additives. (**e**) Buffer 2. Various [Mg^{2+}] in the absence and presence of dNTPs (1.4 mM), 70°C. (**f**) Buffers S. Various [Mg^{2+}] in the absence and presence of dNTPs (1.4 mM), 70 °C. *Tt*Ago: guide: target =5: 1: 1. N=3.

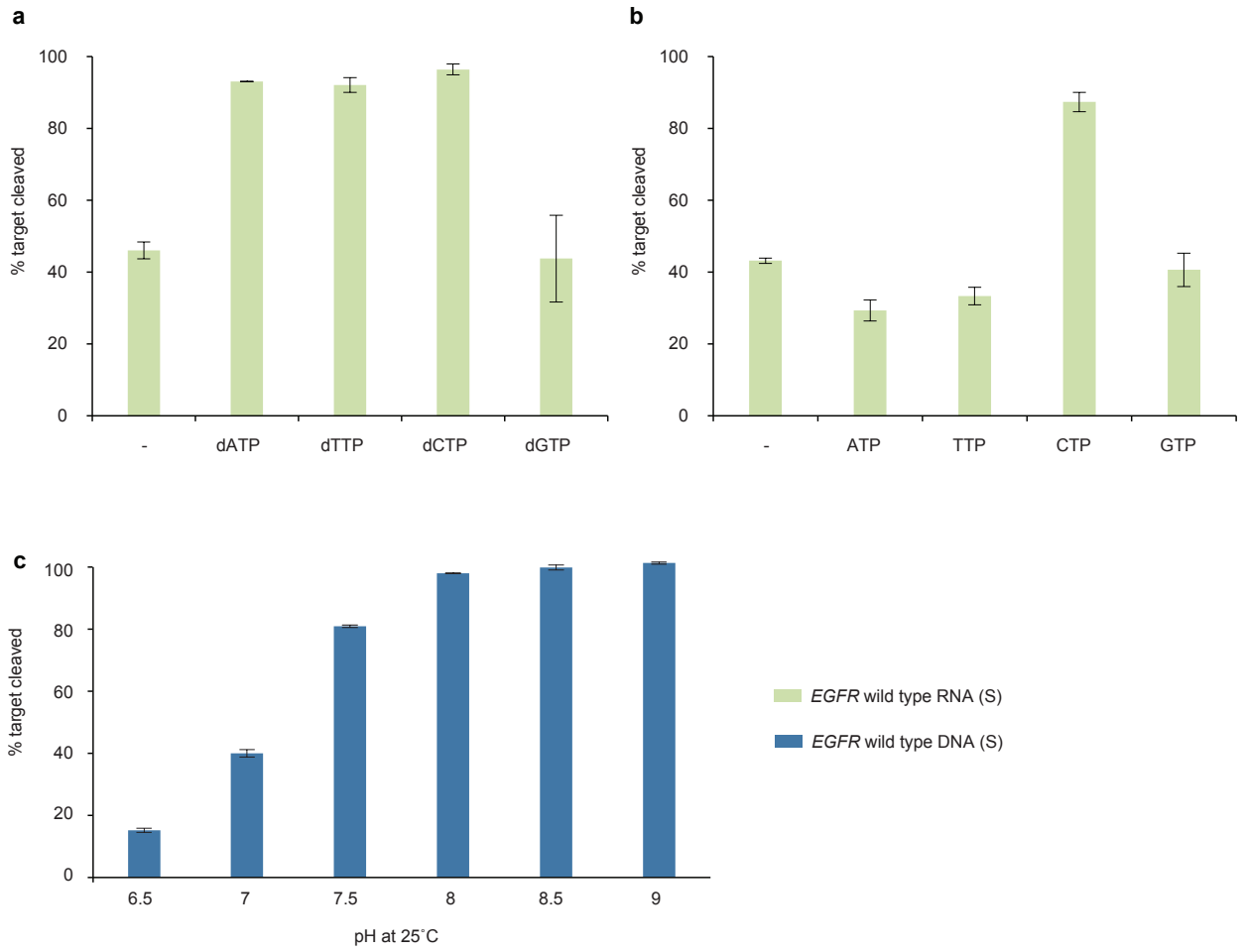

Supplementary Figure 5: The effects of **(a)** dNTPs and **(b)** NTPs on *EGFR* RNA (S) cleavage with guide *EGFR* (L858R)-S (16nt)-MP10 at 80°C. **(c)** The effect of pH on *EGFR* DNA (S) cleavage with guide *EGFR* (L858R)-S (16nt)-MP10 at 75 °C. *Tt*Ago: guide: target =5: 1: 1. N=3.

Supplementary Section 2: The effect of guide DNA mismatch position on cleaving efficiency

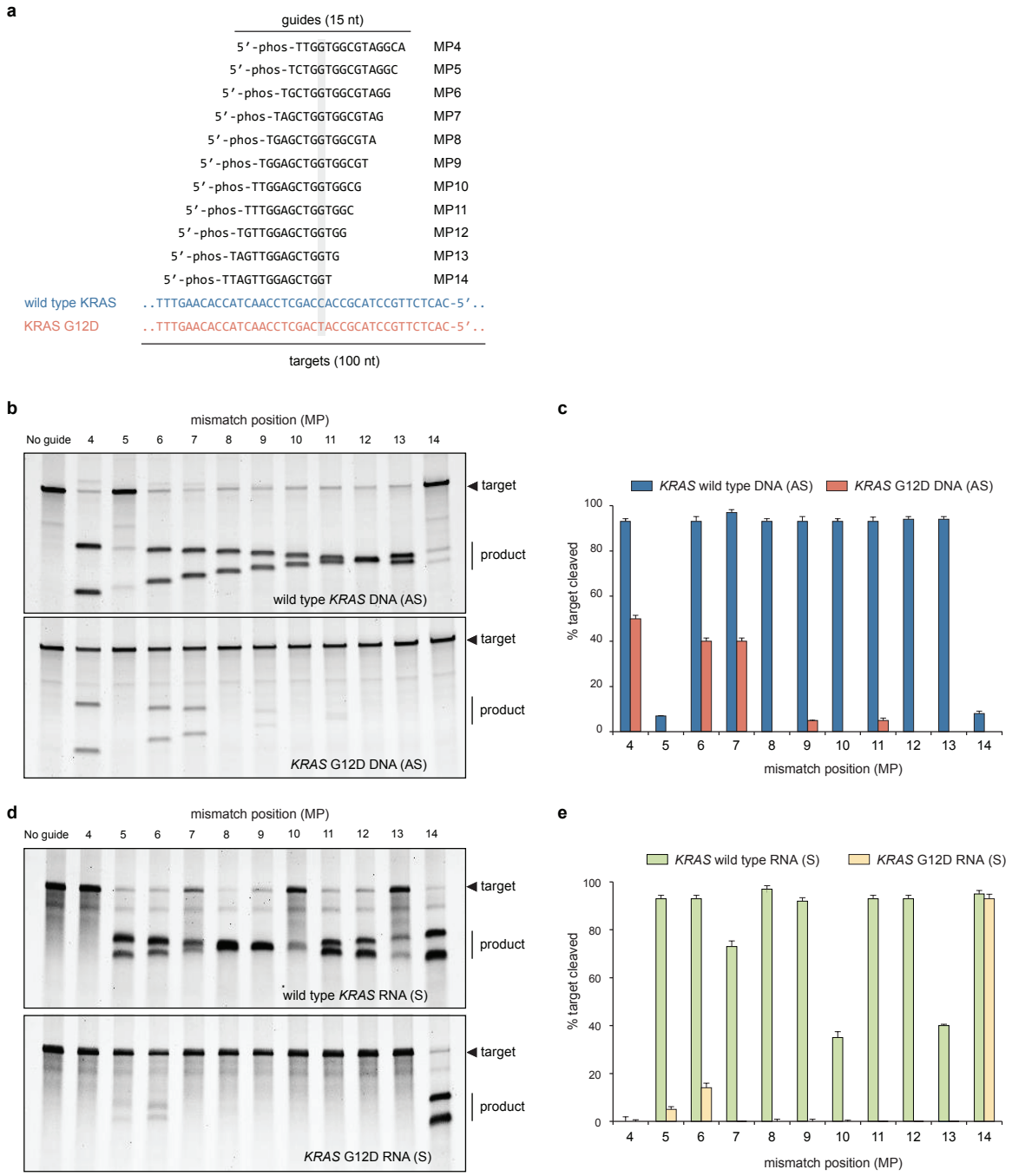

Supplementary Figure 6: Cleavage efficiencies of WT *KRAS* and *KRAS* G12D DNA and RNA as functions of MP. (**a**) *KRAS* – antisense (AS) guide and AS target sequences. (**b**) Electropherograms of cleaved AS WT *KRAS* and AS *KRAS* G12D DNA strands (80°C, 20 min). (**c**) Cleaving efficiencies of AS *KRAS* WT and AS *KRAS* G12D DNA as functions of MP. (**d**) Electropherograms of cleaved WT *KRAS* RNA and *KRAS* G12D RNA (80°C, 20 min) (**e**) Cleaving efficiencies of WT *KRAS* RNA and *KRAS* G12D RNA as functions of MP. *Tt*Ago: guide: target =5: 1: 1. N=3. The sequences of guides and synthetic targets are listed in Supplementary Note 1.

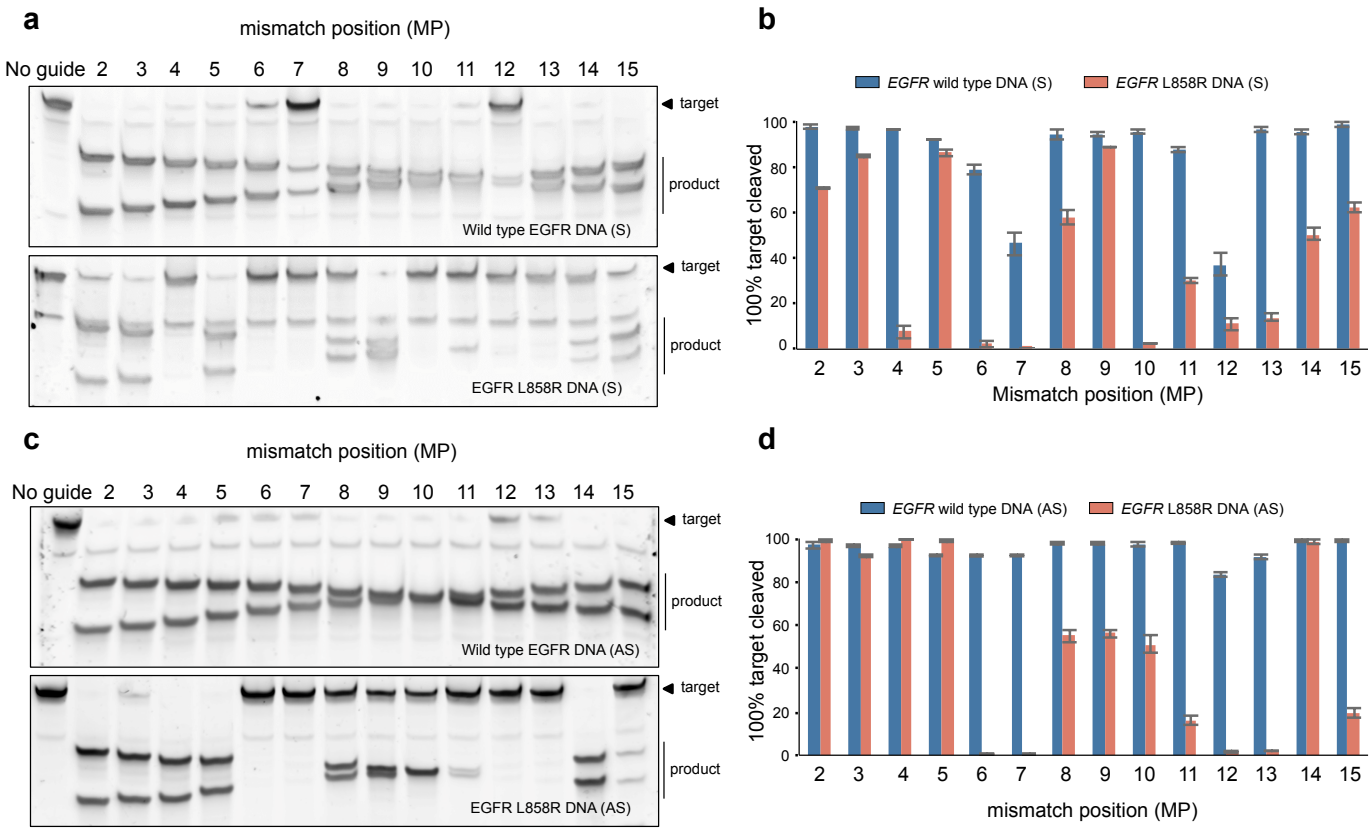

Supplementary Figure 7: Cleavage efficiencies of WT *EGFR* and *EGFR* L858R DNA as functions of MP. (**a**) Electropherograms of incubation products (80°C, 20 min) of WT *EFGR* and *EFGR* L858R DNA S strands. (**b**) Cleaving efficiencies of S WT *EFGR* and S *EFGR* L858R DNA strands as functions of MP. (**c**) Electropherograms of incubation products (80°C, 20 min) of AS WT *EFGR* and AS *EFGR* L858R DNA strands. (**d**) Cleaving efficiencies of AS WT *EFGR* and AS *EFGR* L858R DNA strands as functions of MP. *Tt*Ago: guide: target =5: 1: 1. N=3. The sequences of guides and synthetic targets are listed in Supplementary Note 1.

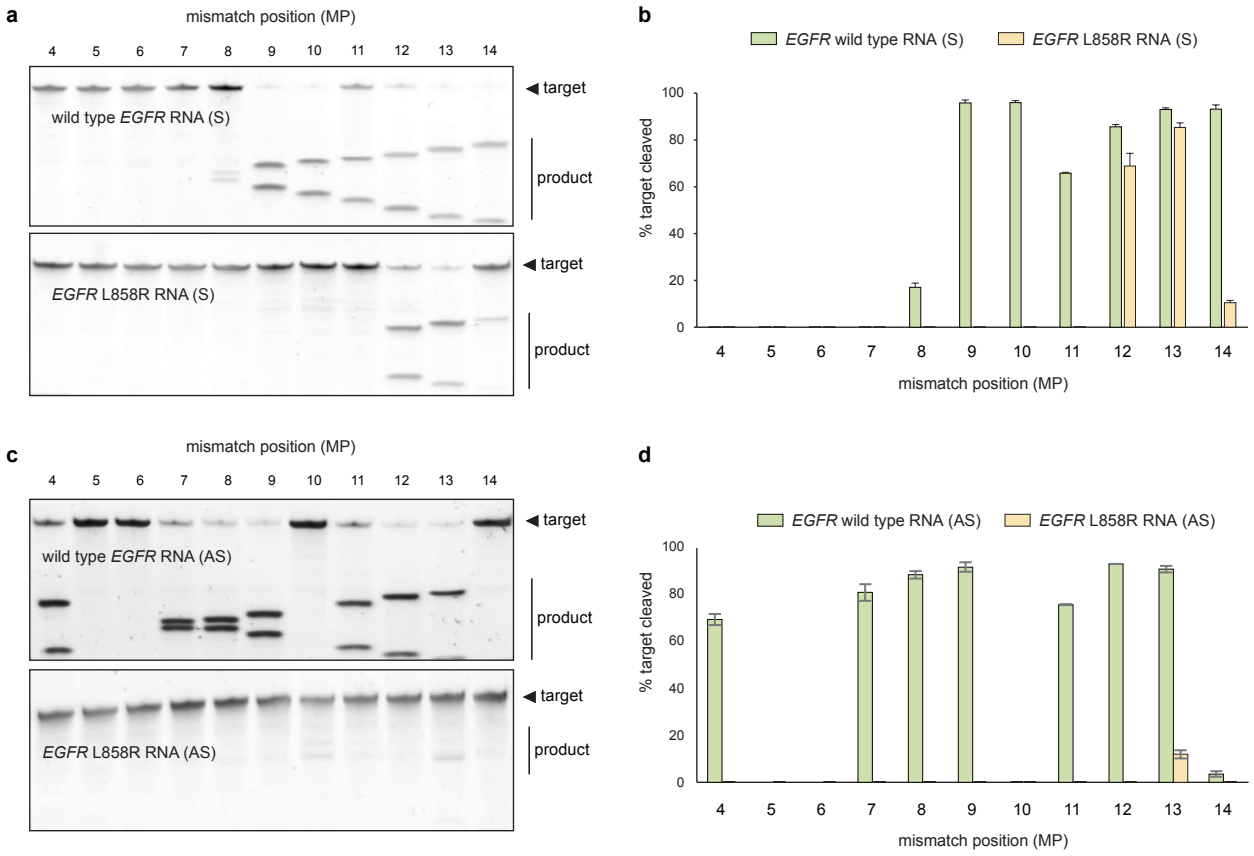

Supplementary Figure 8: Cleavage efficiencies of WT *EGFR* and *EGFR* L858R MA RNA as functions of the position of the mismatched pair (MP). (**a**) Electropherograms of incubation products (80°C, 20 min) of S WT *EFGR* and S *EFGR* L858R RNA strands. (**b**) Cleaving efficiencies of S WT *EFGR* and S *EFGR* L858R RNA strands as functions of MP. (**c**) Electropherograms of incubation products (80°C, 20 min) of AS WT *EFGR* and AS *EFGR* L858R RNA strands. (**d**) Cleaving efficiencies of AS WT *EFGR* and AS *EFGR* L858R RNA strands as functions of MP. *Tt*Ago: guide: target =5: 1: 1. N=3. The sequences of guides and synthetic targets are listed in Supplementary Note 1.

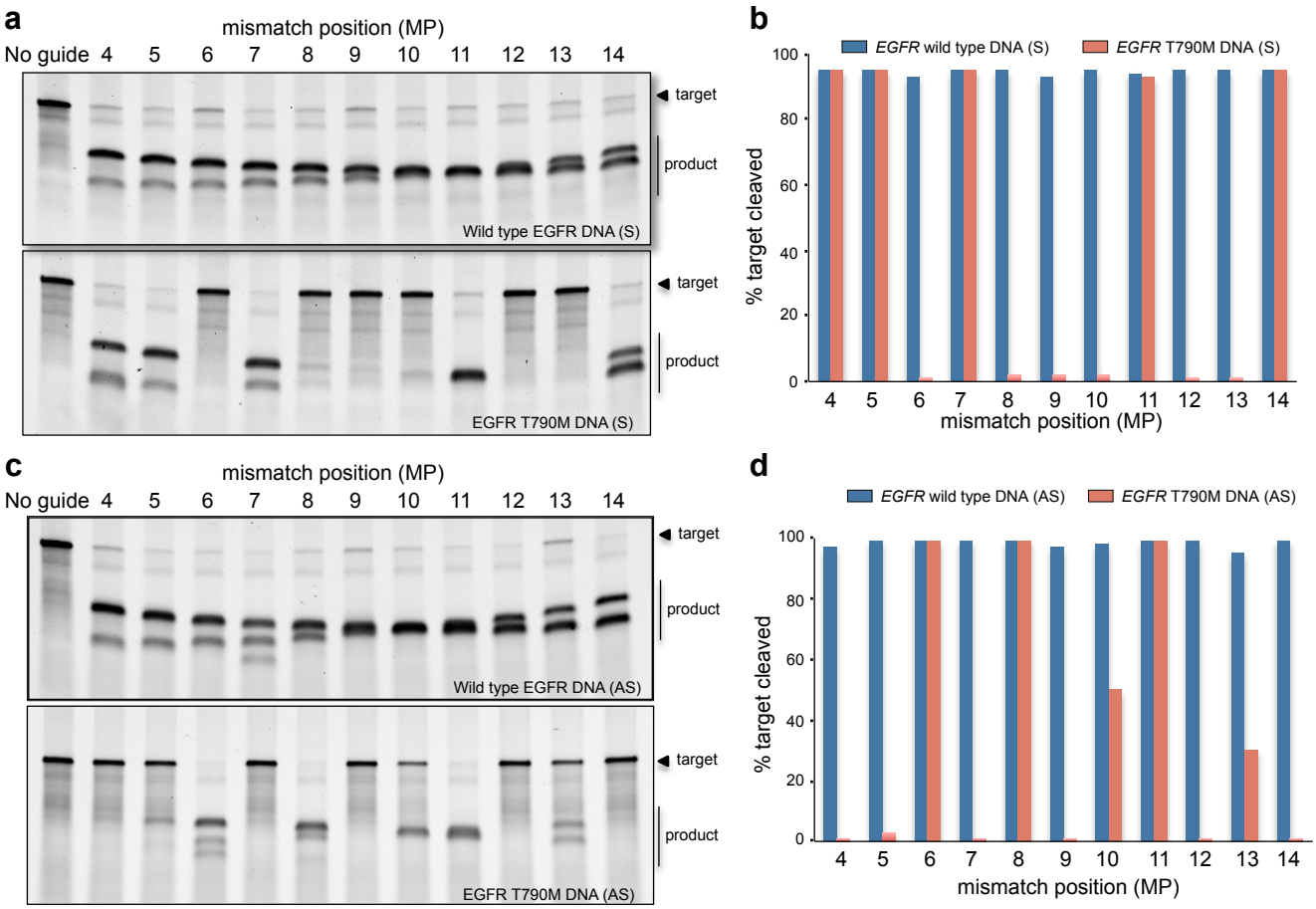

Supplementary Figure 9: Cleavage efficiencies of WT *EGFR* and *EGFR* T790M DNA as functions of the position of the mismatched pair. (**a**) Electropherograms of incubation products (80°C, 20 min) of S WT *EFGR* and S *EFGR* T790M DNA strands. (**b**) Cleaving efficiencies of S WT *EFGR* and S *EFGR* T790M DNA strands as functions of MP. (**c**) Electropherograms of incubation products (80°C, 20 min) of AS WT *EFGR* and AS *EFGR* T790M DNA strands. (**d**) Cleaving efficiencies of AS WT *EFGR* and AS *EFGR* T790M DNA strands as functions of MP. *Tt*Ago: guide: target =5: 1: 1. The sequences of guides and synthetic targets are listed in Supplementary Note 1.

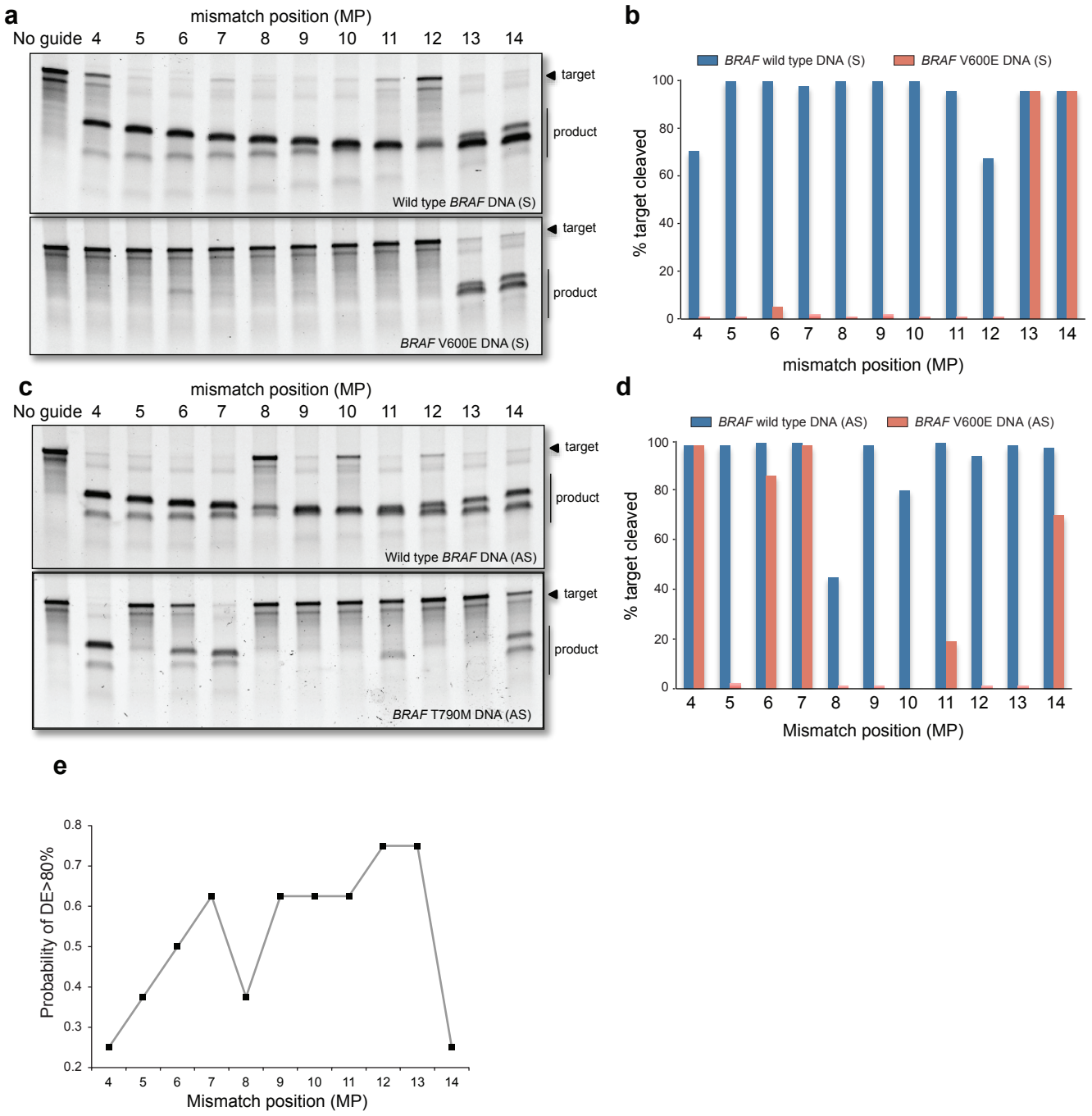

Supplementary Figure 10: Cleavage efficiencies of WT *BRAF* and *BRAF* V600E DNA as functions of the position of the mismatched pair between *BRAF* guide and *BRAF* V600E. (**a**) Electropherograms of incubation products (80°C, 20 min) of S WT *BRAF* and S *BRAF* V600E DNA strands. (**b**) Cleaving efficiencies of S WT *BRAF* and S *BRAF* V600E DNA strands as functions of MP. (**c**) Electropherograms of incubation products (80°C, 20 min) of AS WT *BRAF* and AS *BRAF* V600E DNA strands. (**d**) Cleaving efficiencies of AS WT *BRAF* and AS *BRAF* V600E DNA strands as functions of MP. (**e**) Probability of discrimination efficiency (DE) >80% as a function of MP for the cases in Fig. 2c. *Tt*Ago: guide: target =5: 1: 1. The sequences of guides and synthetic targets are listed in Supplementary Note 1.

Supplementary Section 3: The effects of guide length and temperature on *Tt*Ago cleavage

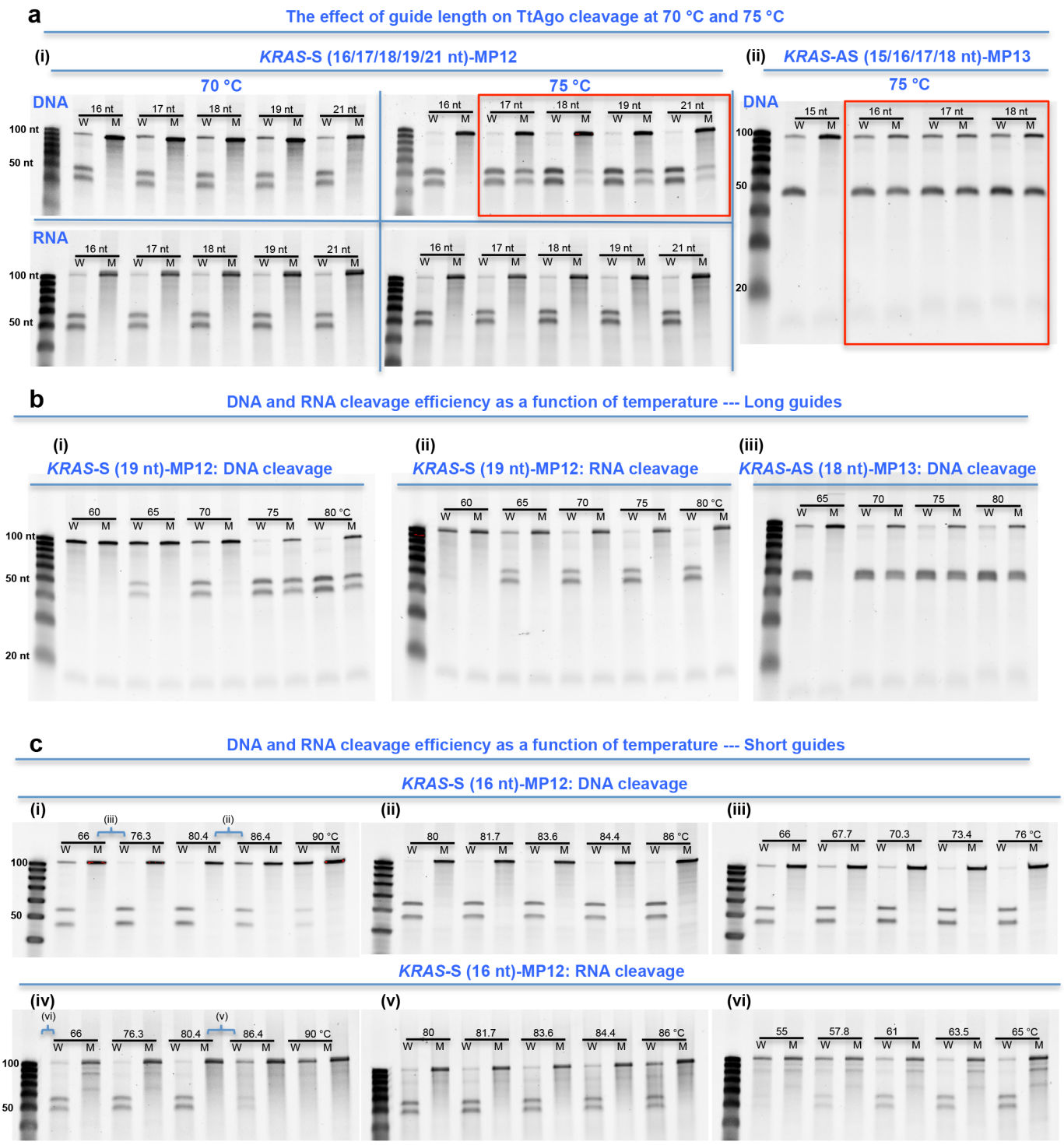

Supplementary Figure 11: *Tt*Ago cleavage as a function of guide length and temperature. (a) Electropherograms of *Tt*Ago cleavage products as functions of guide length at 70 and 75°C. (i) *KRAS* DNA and RNA S strands. (ii) *KRAS* DNA AS strand. (b) Effect of temperature on cleavage efficiency using long (18/19 nt) guides with a guide/mutant allele mismatch at positions 12 (S-*KRAS*) and 13 (AS *KRAS*). (c) *Tt*Ago cleavage of DNA and RNA with a short guide (16 nt) as a function of temperature. *Tt*Ago: guide: target =5: 1: 1. N=3.

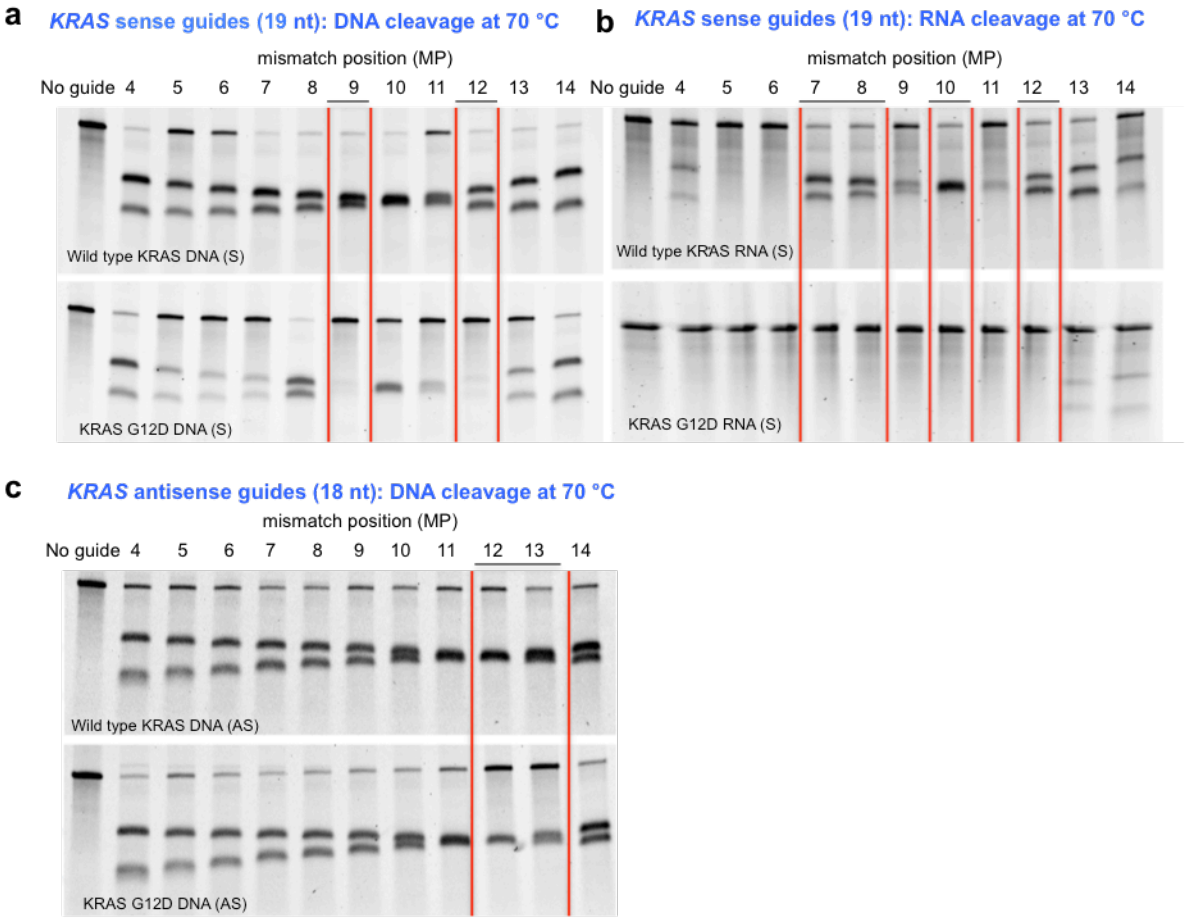

Supplementary Figure 12: Cleavage efficiency of WT *KRAS* and *KRAS* G12D alleles with long guides (18/19 nt) as functions of mismatched pair position. (**a, b**) The cleavage efficiency of DNA (a) and RNA (b) with *Tt*Ago and S *KRAS* 19 nt guide as a function of mismatched pair position at 70°C. (b) The cleavage efficiency of *Tt*Ago with AS *KRAS* 18 nt guides as a function of mismatched pair position at 70°C. *Tt*Ago: guide: target =5: 1: 1. N=3. The sequences of guides and synthetic targets are listed in Supplementary Note 1.

Supplementary Section 4: *Tt*Ago cleavage of dsDNA

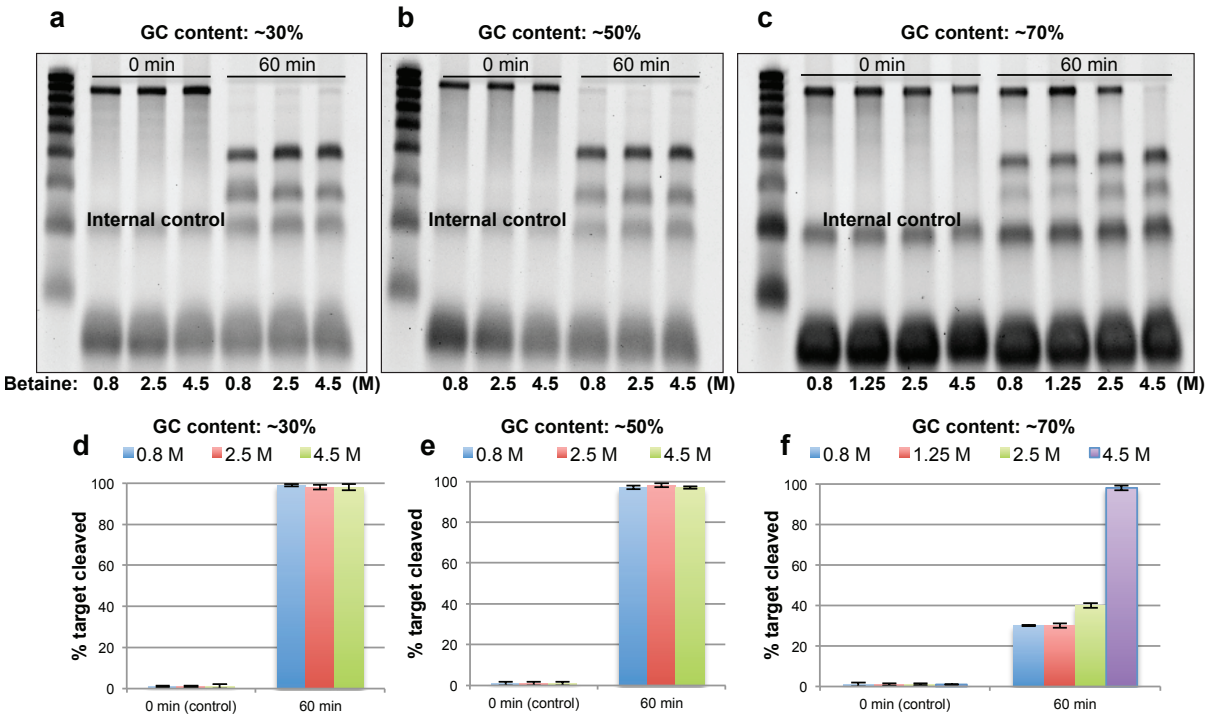

Supplementary Figure 13: The cleavage efficiency of dsDNA with various GC content as a function of betaine concentration. (a, b, c) Electropherograms of cleaving assay products of randomly generated dsDNA (90 bp) with (a) ~30%, (b) ~50%, and ~70% GC content. (**d, e, f**) Cleaving efficiencies corresponding to (a), (b), and (c). The experiments were carried out at 83°C with *Tt*Ago/guides ratio 1 : 10 and indicated betaine concentration. N=3. The sequences of guides and synthetic targets are listed in Supplementary Note 1.

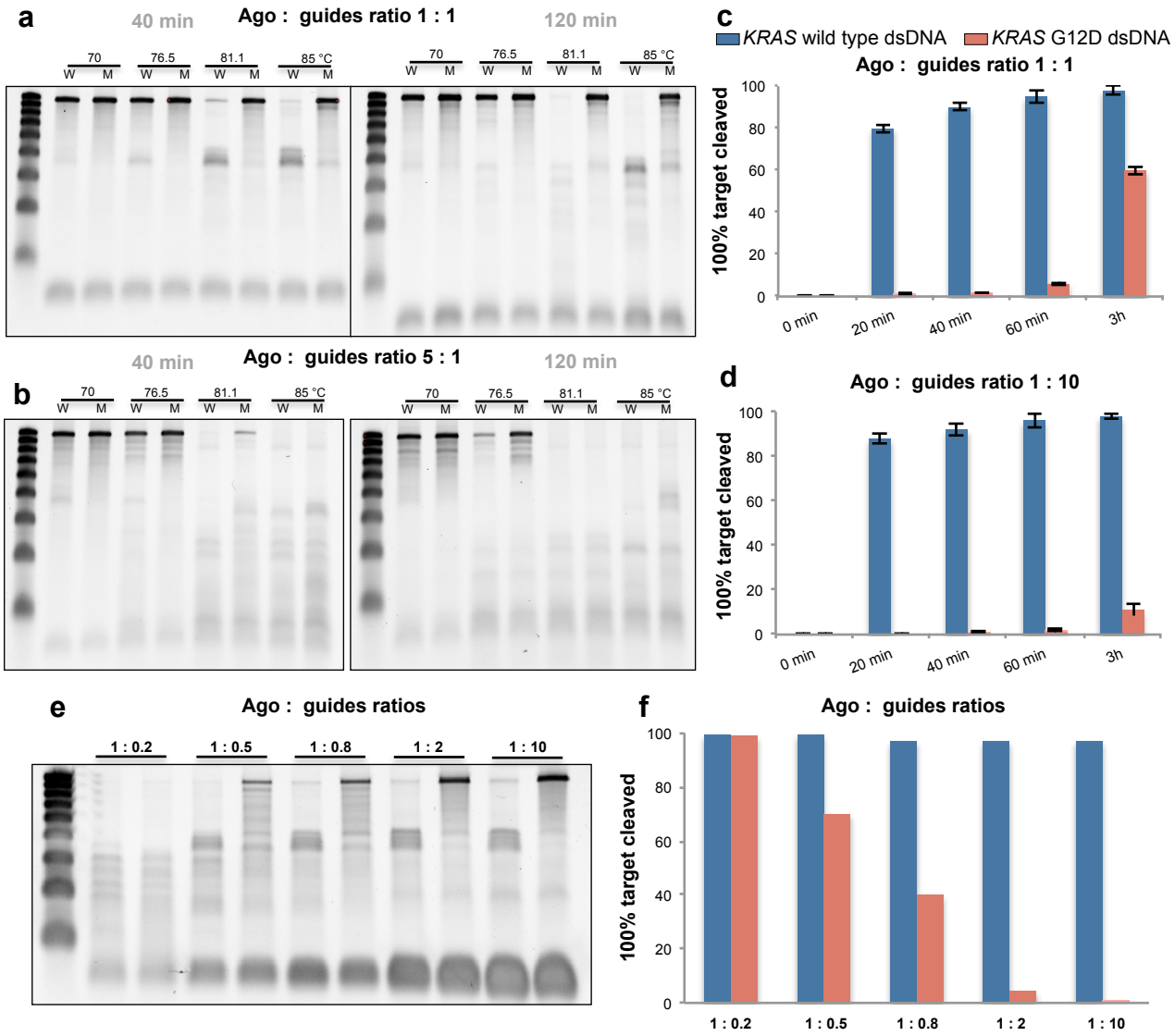

Supplementary Figure 14: dsDNA cleavage efficiency as a function of temperature, guide concentration, and incubation time. (a, b) Electropherograms of ds*KRAS* (100 bp) cleaving assay products corresponding to **Figs. 5a** and **5b**. **(c)** Cleaving efficiency corresponding to Fig. 5c as a function of incubation time at 83°C. *Tt*Ago/guides ratio 1 : 1. N=3. **(d)** Cleaving efficiency corresponding to Fig. 5d as a function of incubation time at 83°C. *Tt*Ago/guides ratio 1: 10. N=3. **(e)** Electropherograms of dsDNA cleavage as a function of *Tt*Ago/guides ratio. Incubation time 1h at 83°C. **(f)** Cleaving efficiency corresponding to (e) as a function of *Tt*Ago/guides ratio. All the experiments were carried out in Buffer 3 with *KRAS*-S (16nt)-MP12 and *KRAS*-AS (15nt)-MP13 guides.

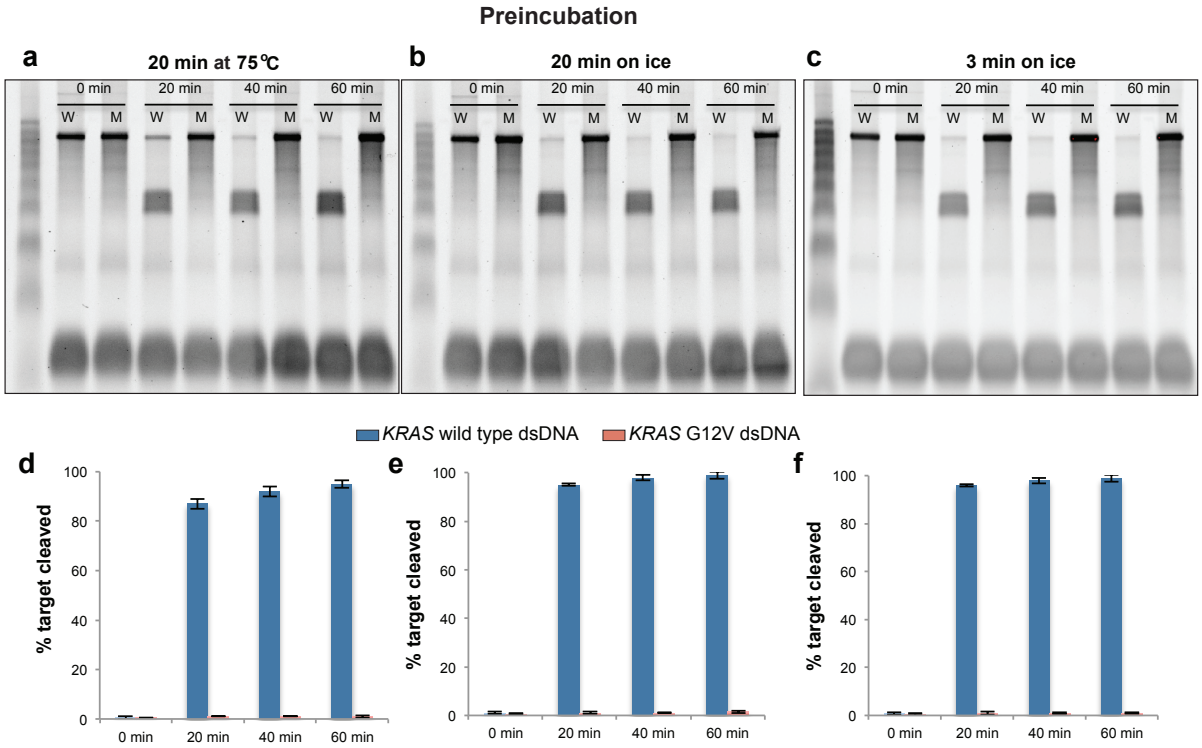

Supplementary Figure 15: dsDNA cleavage efficiency as a function of *Tt*Ago/guide pre-incubation conditions. (a, b, c) Electropherograms of cleaving assay products of ds*KRAS* (100 bp) harboring G12V. *Tt*Ago/guide complex is preincubated (a) at 75°C for 20 min, (b) on ice for 20 min, and (c) on ice for 3 min. **(d, e, f)** Cleaving efficiencies of the assays in (a), (b), (c). All experiments were carried out in Buffer 3 at 83°C with indicated incubation times and with *KRAS*-S (16nt)-MP12 and *KRAS*-AS (15nt)-MP13 guides. *Tt*Ago/guides ratio 1 : 10. N=3.

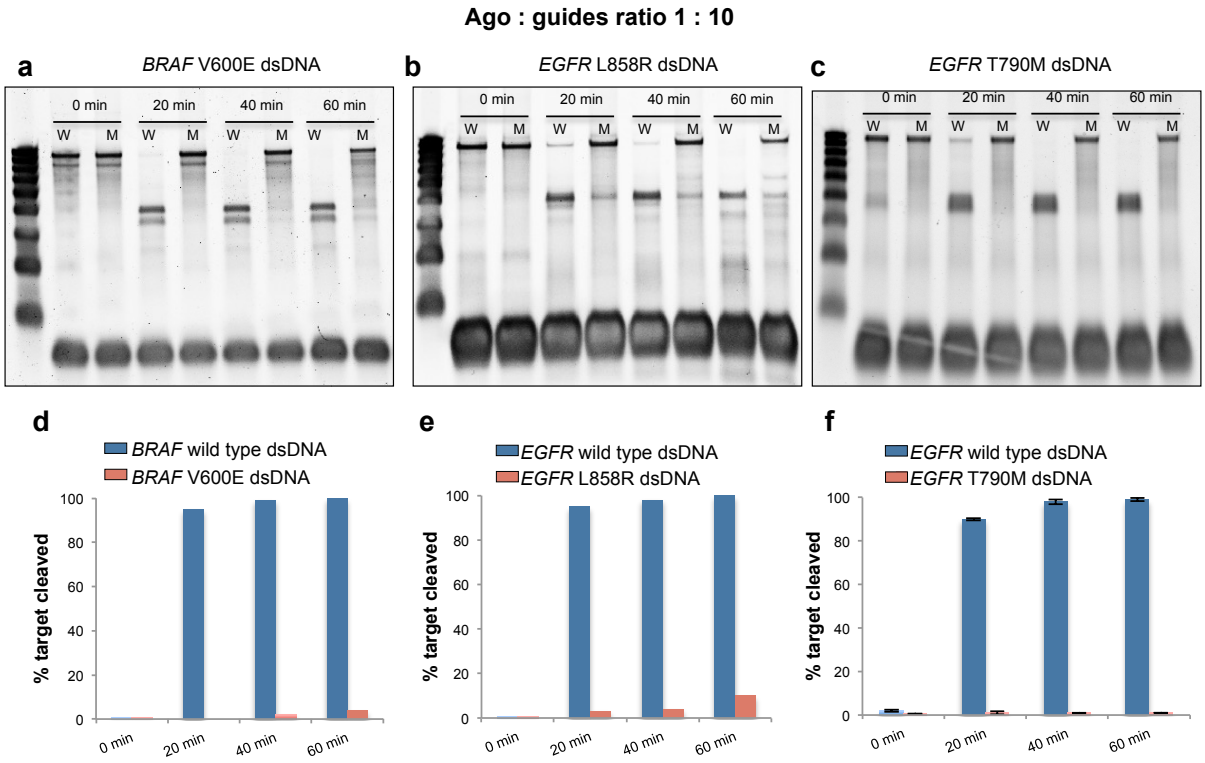

Supplementary Figure 16: dsDNA cleavage efficiency of MAs harboring hotspot point mutations as a function of incubation time. (a) Electropherograms of cleaving assay products of ds*BRAF* (100 bp) with *BRAF*-S (16nt)-MP9 and *BRAF*-AS (16nt)-MP13 guides. **(b)** Electropherograms of cleaving assay products of ds*EGFR* (100 bp) with *EGFR* L858R S (16nt)-MP10 and *EGFR* L858R AS (15nt)-MP7 guides. **(c)** Electropherograms of cleaving assay products of ds*EGFR* (100 bp) with *EGFR* T790M S (16nt)-MP10 and *EGFR* T790M AS (15nt)-MP7 guides. **(d, e, f)** Cleaving efficiencies of the assays in (a), (b), (c). All experiments were carried out at 83°C with indicated incubation times and *Tt*Ago/guides ratio 1 : 10.

a

***EGFR* exon19 deletion mutations**

EGFR deletion (Ed) name	Frequency of EGFR exon19 deletion subtypes	Amino acid change	Base pair change	Length (bp)
Ed1	**45%**	p.E746_ A750del(1)	c.2235_2249del15	65
Ed2	**19.6%**	p.E746_ A750del(2)	c.2236_2250del15	65
Ed3	**8.4%**	p.L747_ P753>S	c.2240_2257del18	62
Ed4	**4.3%**	p.L747_ T751del	c.2240_2254del15	65
Ed5	**3.4%**	p.L747_ A750>P	c.2239_2250>cca	71
Ed6	**3.2%**	p.E746_ S752>V(2)	c.2237_2257>ttc	62
Ed7	**1.6%**	p.E746_ S752>V	c.2237_2255>t	62
Ed8	**1.4%**	p.L747_ S752del	c.2239_2256del18	62

b

```
EGFR deletion mutation-S-guide                    3′-GTTCCTTAATTCTCTT-p
S WT (80bp):       5′-GGTGAGAAAGTTAAAATTCCCGTCGCTATCAAGGAATTAAGAGAAGCAACATCTCCGAAAGCCAACAAGGAAATCCTCGA-3′
S 2235_2249del15:  5′-GGTGAGAAAGTTAAAATTCCCGTCGCTATCAA--------------AACATCTCCGAAAGCCAACAAGGAAATCCTCGA-3′
S 2236_2250del15:  5′-GGTGAGAAAGTTAAAATTCCCGTCGCTATCAAG-------------ACATCTCCGAAAGCCAACAAGGAAATCCTCGA-3′
S 2240_2257del18:  5′-GGTGAGAAAGTTAAAATTCCCGTCGCTATCAAGGAAT-----------CGAAAGCCAACAAGGAAATCCTCGA-3′
S 2240_2254del15:  5′-GGTGAGAAAGTTAAAATTCCCGTCGCTATCAAGGAAT-------------CTCCGAAAGCCAACAAGGAAATCCTCGA-3′
S 2239_2250>cca:   5′-GGTGAGAAAGTTAAAATTCCCGTCGCTATCAAGGAA----CCA-----ACATCTCCGAAAGCCAACAAGGAAATCCTCGA-3′
S 2237_2257>ttc:   5′-GGTGAGAAAGTTAAAATTCCCGTCGCTATCAAGG------TTC-----------CGAAAGCCAACAAGGAAATCCTCGA-3′
S 2237_2255>t:     5′-GGTGAGAAAGTTAAAATTCCCGTCGCTATCAAGG-------T----------TCCGAAAGCCAACAAGGAAATCCTCGA-3′
S 2239_2256del18:  5′-GGTGAGAAAGTTAAAATTCCCGTCGCTATCAAGGAA----------------CCGAAAGCCAACAAGGAAATCCTCGA-3′

EGFR deletion mutation-AS-guide                          p-TAAGAGAAGCAACATC-3′
AS WT (80bp):      3′-CCACTCTTTCAATTTTAAGGGCAGCGATAGTTCCTTAATTCTCTTCGTTGTAGAGGCTTTCGGTTGTTCCTTTAGGAGCT-5′
AS 2235_2249del15: 3′-CCACTCTTTCAATTTTAAGGGCAGCGATAGTT--------------TTGTAGAGGCTTTCGGTTGTTCCTTTAGGAGCT-5′
AS 2236_2250del15: 3′-CCACTCTTTCAATTTTAAGGGCAGCGATAGTTC-------------TGTAGAGGCTTTCGGTTGTTCCTTTAGGAGCT-5′
AS 2240_2257del18: 3′-CCACTCTTTCAATTTTAAGGGCAGCGATAGTTCCTTA----------GCTTTCGGTTGTTCCTTTAGGAGCT-5′
AS 2240_2254del15: 3′-CCACTCTTTCAATTTTAAGGGCAGCGATAGTTCCTTA-------------GAGGCTTTCGGTTGTTCCTTTAGGAGCT-5′
AS 2239_2250>cca:  3′-CCACTCTTTCAATTTTAAGGGCAGCGATAGTTCCTT----GGT-----TGTAGAGGCTTTCGGTTGTTCCTTTAGGAGCT-5′
AS 2237_2257>ttc:  3′-CCACTCTTTCAATTTTAAGGGCAGCGATAGTTCC------AAG-----------GCTTTCGGTTGTTCCTTTAGGAGCT-5′
AS 2237_2255>t:    3′-CCACTCTTTCAATTTTAAGGGCAGCGATAGTTCC-------A----------AGGCTTTCGGTTGTTCCTTTAGGAGCT-5′
AS 2239_2256del18: 3′-CCACTCTTTCAATTTTAAGGGCAGCGATAGTTCCTT----------------GGCTTTCGGTTGTTCCTTTAGGAGCT-5′
```

c

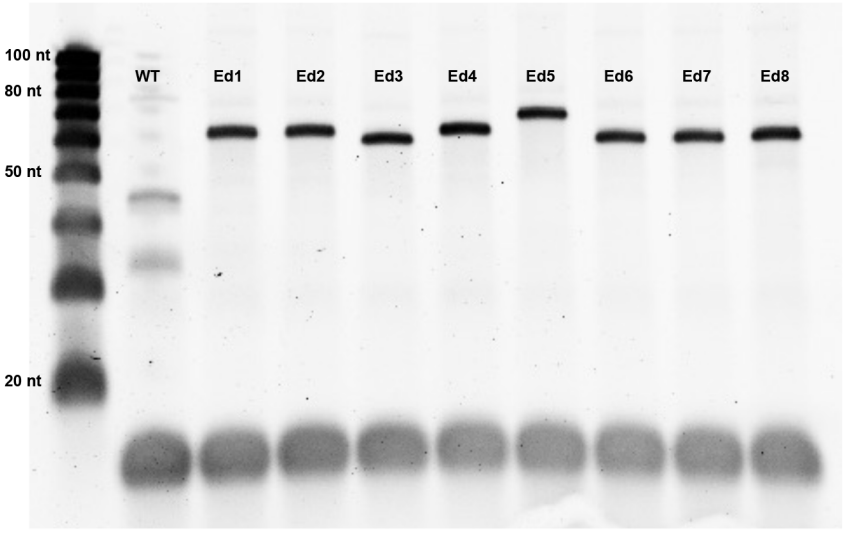

Supplementary Figure 17: NAVIGATER's enriches MAs harboring deletion mutations. (a) Common *EGFR* exon19 deletion mutations(9). **(b)** Targets and guides sequences. ds*EGFR*. **(c)** Electropherograms of cleaving assay products of ds*EGFR*. Incubation time 1 hour at 83°C. *Tt*Ago/guides ratio 1: 10.

Supplementary Section 5: CRISPR/Cas9-based dsDNA cleavage

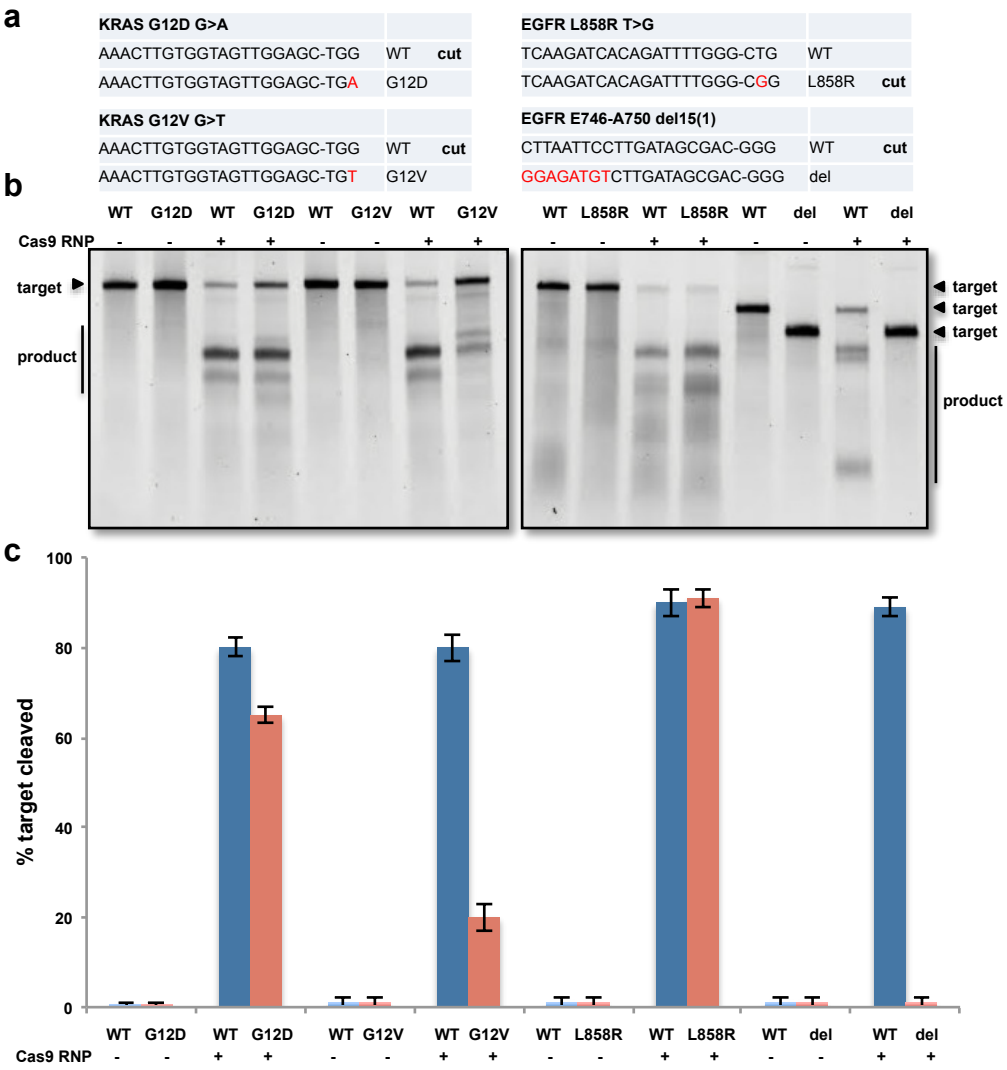

Supplementary Figure 18: CRISPR-Cas9 based dsDNA cleavage. (a) The crRNA sequences used for ds*KRAS* and ds*EGFR* cleavage. **(b)** Electropherograms of ds*KRAS* (100 bp) and ds*EGFR* (100 bp) cleaving assay products. CRISPR/Cas9 nonspecifically cleaved ds*KRAS* harboring G12D and G12V mutation and ds*EGFR* harboring L858R mutation, but specifically cleaved WT ds*EGFR* while sparing ds*EGFR* harboring deletion mutation E746-A750 del [1]. (**c**) Cleaving efficiency of the assay in (b). N=3

Supplementary Section 6: NAVIGATER improves the sensitivity of downstream rare allele detection

Supplementary Table 2. The genotype and mutation frequency of 6 samples from pancreatic cancer patients*						
Patient number	**P1**	**P2**	**P3**	**P4**	**P5**	**P6**
Genotype and mutation fraction*	NC**	NC**	G12R 3%	G12V 5%	G12D 0.5%	G12D 20%
* Samples were analyzed with standard ddPCR protocol(10). ** Negative control, blood collected from healthy volunteer. All samples contain similar numbers of WT-*KRAS* (s.d. <10%). See Supplemental Fig. 20b.						

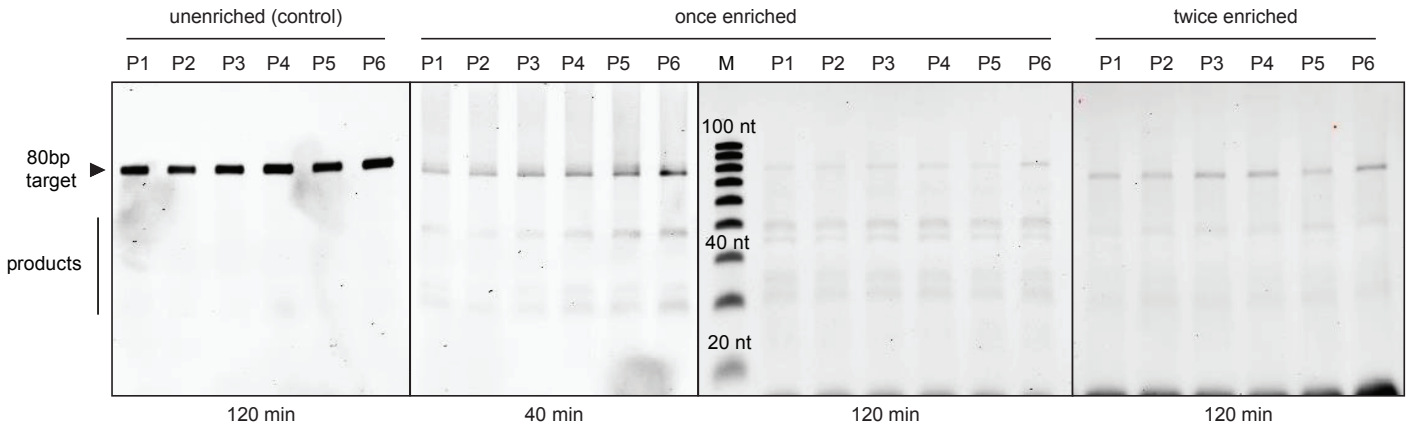

Supplementary Figure 19: Electropherograms of six pancreatic cancer patient's samples (Supplementary Table 2) without enrichment (control), once enriched for 40 and 120 min, and twice-enriched.

Supplementary Table 3: The sequences and concentrations of *KRAS* primers, PNA clamp oligo, and Taqman probes used in downstream mutation analysis.		
Name	Sequences (5'---3')	Concentration
KRAS ddPCR-FW (10)	AGGCCTGCTGAAAATGACTGAATAT	400/100 nM
KRAS ddPCR-RV (10)	GCTGTATCGTCAAGGCACTCTT	400/100 nM
G12-WT-VIC probe (10)	TTGGAGCTGGTGGCGT	100 nM
G12D-FAM probe (10)	TGGAGCTGATGGCGT	100 nM
G12R-FAM probe (10)	TTGGAGCTCGTGGCGT	100 nM
G12V-FAM probe (10)	ACGCCAACAGCTC	100 nM
KRAS RT-PCR-FW (11)	ATTTCGGACTGGGAGCGAGC	100 nM
KRAS RT-PCR-RV (11)	GTCCCTCATTGCACTGTACTC	100 nM
SMAP-2-OP1	AGGCCTGCTGAAAATGA	0.4 μM
SMAP-2-OP2 (1)	TTGGATCATATTCGTCC	0.4 μM
SMAP-2-FP (1)	ACCTTCTACCCTCAGAAGGTATAAACTTGTG GTAGTTGGAGC	3.0 μM
SMAP-2-BP (1)	GCAAGAGTGCCTTGA	1.5 μM
SMAP-2-TP (1)	TGGCGTAGGCATGATTCTGAATTAGCTGTAT	3.0 μM
PNA clamp (1)	CCTACGCCACCAGCTCC	0.7 μM

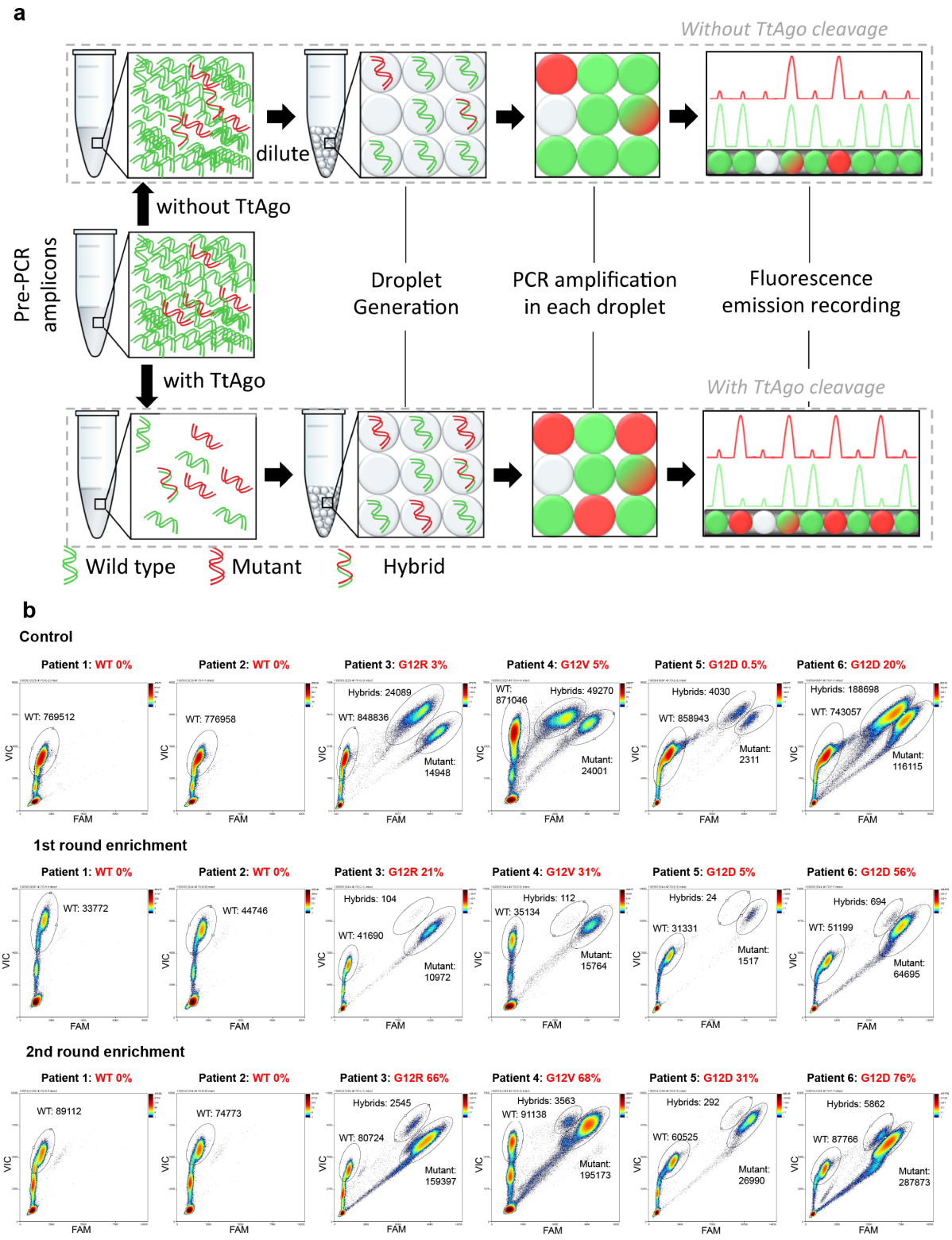

Supplementary Figure 20: Six pancreatic cancer patient's samples processed with NAVIGATER plus ddPCR. (**a**) Principle of operation of NAVIGATER combined with ddPCR. (**b**) ddPCR results of non-enriched, once-enriched, and twice-enriched samples. There are three signaling droplet populations for *KRAS*: WT, mutant, and WT-mutant hybrid. 2~7 millions of droplets are produced for each sample.

Supplementary Section 7: Multiplexed enrichment

We carried out triplex NAVIGATER with 3 different pairs of guides to enrich samples of 60 ng Horizon standard cfDNA harboring various MAF of *KRAS* G12D, *EGFR* L858R, and *EGFR* ΔE746 - A750 mutations. We compared the triplex NAVIGATER products with triplex Cas9 -based DASH (Cas9-DASH) (12) (Supplementary Figs. 21, 22). In the absence of *Tt*Ago treatment (control), the electropherograms of triplex PCR and single-plex (reference) products feature five bands: at ~120 bp (predominantly WT *KRAS* G12D amplicon); at ~100 bp (predominantly, WT *EGFR* sequence susceptible to L858R mutation and WT *EGFR* sequence susceptible to ΔE746 - A750 mutation; at ~75 bp (internal control); at ~30 bp (Taqman probe); and at ~16 nt (DNA guide) (Supplementary Fig. 21c). After 1 hour incubation, with NAVIGATER and Cas9-DASH, the bands at ~120 bp and ~100 bp faded, indicating a reduction in the concentrations of WT *KRAS* and WT *EGFR* alleles, while there is no change in the band intensities of the internal control (Supplementary Figs. 21a, b). The one-to-one correspondence between the electrophrograms of the triplex assays and single plex assays indicates that there is no interference among guides, and that both NAVIGATER and cas9-DASH are amenable to multiplexing.

To evaluate the performance of these two enrichment assay, enrichment products were subjected to the clamped assay: XNA-PCR (13) that suppresses amplification of WT alleles, enabling detection of mutant alleles down to 0.1% MAF. Without pre-enrichment, XNA-PCR detected down to 0.1% *KRAS* G12D (Supplementary Fig. 22a), 0.1% *EGFR* ΔE746 - A750 (Supplementary Fig. 22g), and 1% *EGFR* L858R (Supplementary Fig. 22d). With NAVIGATER pre-treatment, XNA-PCR sensitivity increased by over 10 folds to 0.01% *KRAS* G12D (Supplementary Fig. 22b), 0.01% *EGFR* ΔE746 - A750 (Supplementary Fig. 22h), and 0.1% *EGFR* L858R (Supplementary Fig. 22e). In contrast, XNA-PCR performed with Cas9-DASH enrichment didn't differ significantly from native XNA-PCR for *KRAS* G12D and *EGFR* L858R (Supplementary Fig. 22c, f), probably due to CRISPR/Cas9's nonspecific cleavage of these two mutant alleles (Supplementary Fig. 18). In summary, NAVIGATER can operate as a multiplexed assay, enriching multiple mutant alleles; it is more specific than CRISPR/Cas9's PAM site recognition-based enrichment; and it can be combined with XNA-PCR to significantly improve XNA-PCR sensitivity.

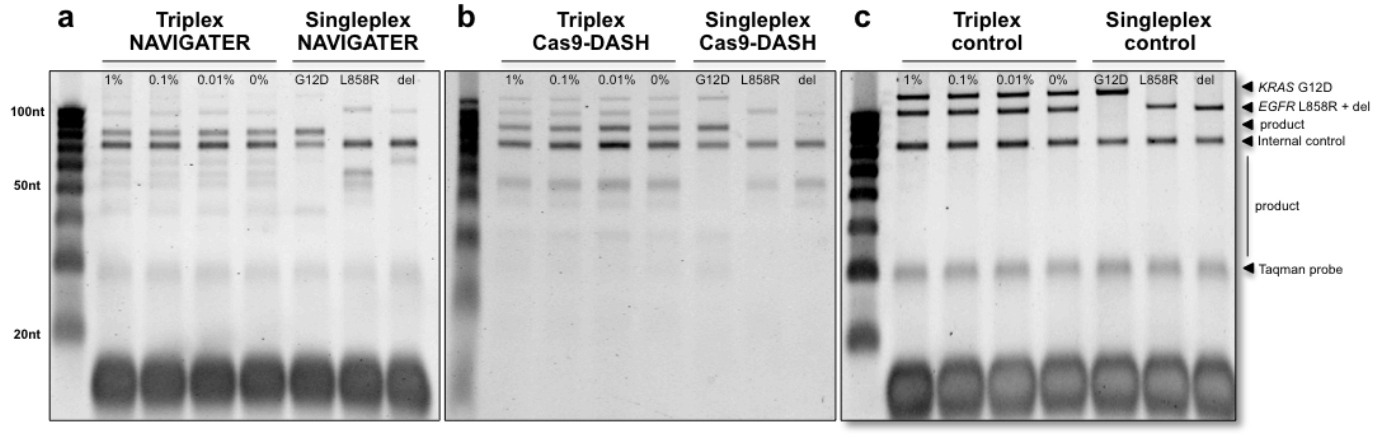

Supplementary Figure 21: Multiplexed enrichment of *KRAS* G12D, *EGFR* L858R, and *EGFR* del (ΔE746 - A750). Electropherograms of PCR products of (**a**) triplex and single-plex NAVIGATER pre-enrichment; (**b**) triplex and single-plex Cas9-DASH pre-enrichment; and (**c**) controls (without enrichment). Single-plex NAVIGATER, single-plex Cas9-DASH, and no-enrichment control are provided as references.

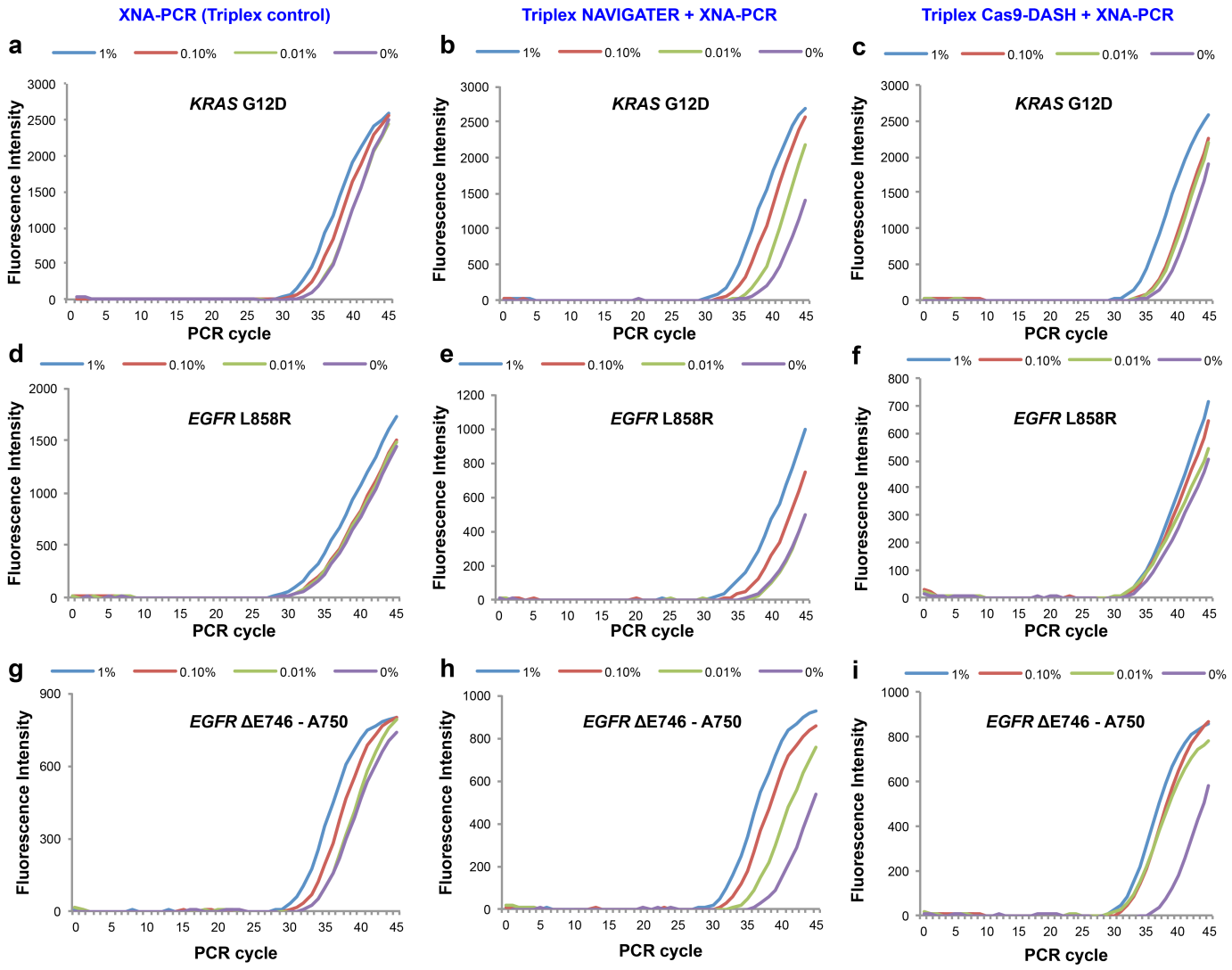

Supplementary Figure 22: Multiplexed enrichment of *KRAS* G12D, *EGFR* L858R, and *EGFR* ΔE746 - A750 with triplex NAVIGATER and cas9-DASH. XNA-PCR amplification curves of samples with various fractions of *KRAS* G12D, *EGFR* L858R and *EGFR* ΔE746 - A750 in the absence (a, d, g) of pre-enrichment (control), presence (b, e, h) of triplex NAVIGATER pre-enrichment, and presence (c, f, i) of triplex Cas9-DASH pre-enrichment. Triplex NAVIGATER shows better enrichment capability than triplex Cas9-DASH. N=3.

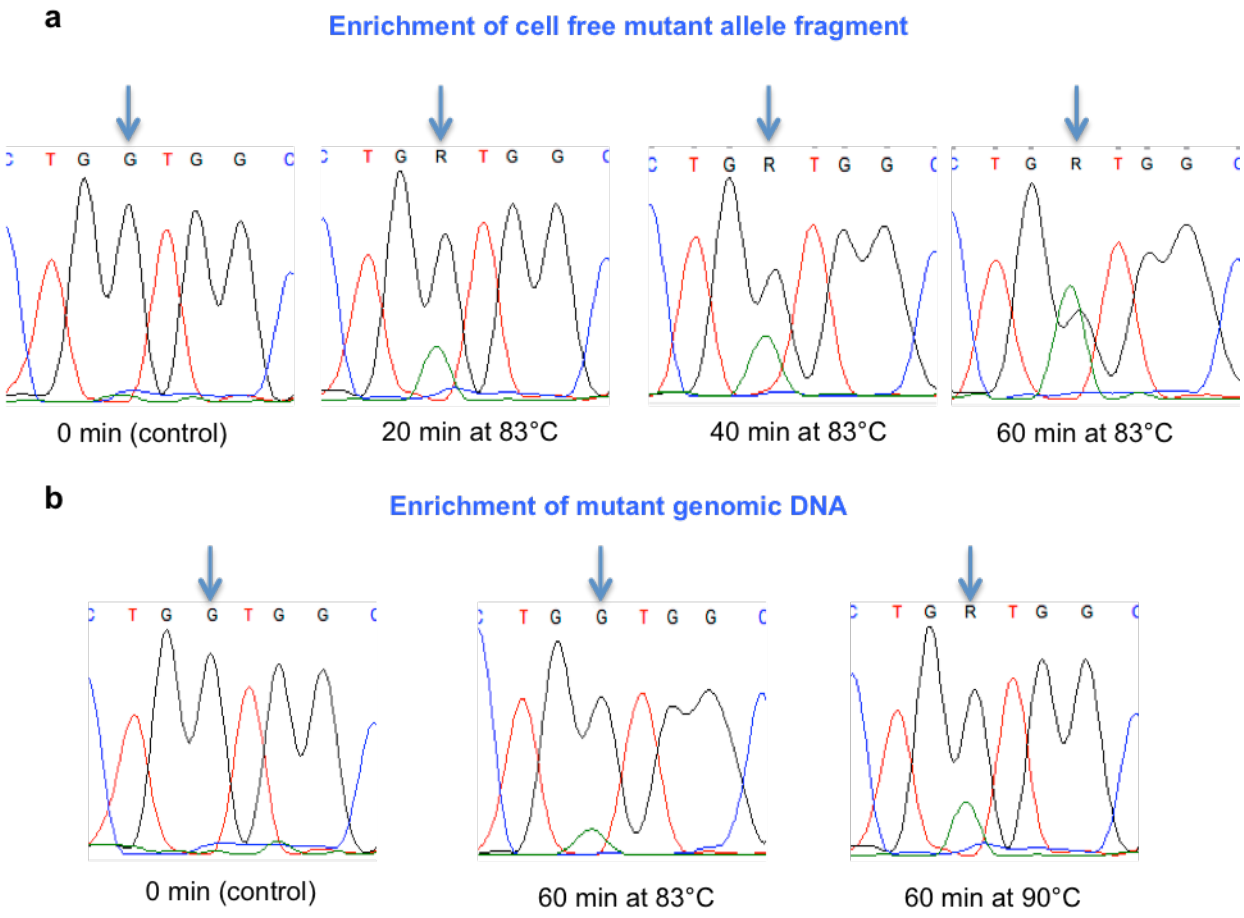

Supplementary Figure 23: NAVIGATER directly enriches *KRAS* G12D mutant allele from cell free DNA fragments and genomic DNA. Sanger sequencing results after NAVIGATER enrichment of (**a**) cell free mutant DNA fragment as a function of incubation (83°C) time and (**b**) mutant genomic DNA as a function of incubation temperature. 60 ng 5% MAF cell-free DNA or genomic DNA (standard cfDNA, Horizon) was added into NAVIGATER to form 10 µL reaction volumes. 4 µL of the products were used for downstream analysis. Guide DNAs were removed by exonuclease 1 before preparing PCR amplicons for Sanger sequencing. N=3.

Supplementary Section 8: Detection methods of low-frequency (<0.2%) cancer mutations in clinical cell-free DNA

XNA-PCR Cut-off threshold cycle (Ct_C). The XNA-PCR vendor (13) recommends Ct_C values for un-enriched samples in the absence of pre-amplification to discriminate against false positives. Since our experimental conditions differ from the manufacturer's protocol, we need to establish new Ct_C for our enriched assays. To this end, we subjected sets of Horizon standard cfDNA samples (N=5, 60ng) without any mutant alleles to XNA-PCR [1] directly without any prior enrichment, [2] after cas9-DASH, [3] once-NAVIGATER, and [4] twice-NAVIGATER. We tailored our calibration samples so that the nucleic acid concentrations in each standard sample exceeds the highest in any of our clinical samples (53.4 ng). In each case, we determined the average Ct and the standard deviation SD. For each assay, we conservatively set Ct_C as the average Ct obtained in our experiments minus 3SD, which provides 99.5% confidence interval against false positives. The Ct_C values for each of our assays are documented at the bottom of Supplementary Table 5. To test our selected Ct_C, we tested calibrated samples Horizon standard cfDNA with 0.01%, 0.1%, and 1% KRAS G12D mutant alleles. In all cases (except 0.01% XNA PCR in the absence of enrichment), the tests were positive.

Receiver Operating Characteristic (ROC) Curves. We calculated the clinical sensitivity and specificity of XNA-PCR only, cas9-DASH XNA-PCR, once-NAVIGATER XNA-PCR, and twice-NAVIGATER XNA-PCR against tissue NGS genotyping results using the threshold Ct as classifier (Fig. 6e and Supplementary Fig. 23).

Sanger sequencing primer. We used the reverse PCR primer 5'-TTGGATCATATTCGTCC-3' to carry out Sanger sequencing of *KRAS* G12 XNA-PCR products. See Supplementary Figure 24 for Sanger sequencing results.

Supplementary Table 4: Patient Samples Tested

(18 pancreatic cancer patients and 4 healthy control donors)

Blinded Sample ID	ALU115 Conc (ng/μL)	Total DNA input (ng)	MAF (%) (ddPCR)	Number of mutant molecule (ddPCR)	Blood mutation type (ddPCR)	Tissue mutation type (Tissue-NGS)	Once NAVIGATER XNA-PCR	Twice NAVIGATER XNA-PCR
01	3.56	53.4	ND			WT		
02	1.28	19.2	ND			WT		
03	0.39	5.9	0.98%	19 copies	G12D	G12D	++++	++++
04	0.08	1.2	ND			G12D		
05	0.50	7.5	0.14%	3.5 copies	G12V	G12V		++
06	1.32	19.8	0.01%	0.66 copies	G12V	G12V		
07	0.56	8.4	0.10%	2.8 copies	G12V	G12V	++++	++++
08	0.62	9.3	ND			NA*		
09	0.17	2.6	ND			G12D	++	++
10	1.01	15.2	ND			NA		
11	0.38	5.7	0.19%	3.6 copies	G12D	G12D	+++	+++
12	0.27	4.1	ND			G12V		+
13	3.06	45.9	ND			WT		
14	0.39	5.9	0.05%	0.98 copies	G12R	G12R		
15	0.37	5.6	ND			G12V		
16	0.66	9.9	ND			NA		
17	0.11	1.7	ND			G12V	+++	+++
18	0.67	10.1	ND			NA		
19	1.14	17.1	ND			WT		
20	1.05	15.8	0.14%	7.4 copies	G12R	G12R	++	++
21	0.79	11.9	0.03%	1.2 copies	G12V	G12V		+
22	0.31	4.7	ND			G12R		

"++++", "+++", "++", "+" indicates, respectively, positive when Ct_C <30.5, <32.5, <34.5, <37.2 for twice-NAVIGATER, and <33.5, <35.5, <37.4 for once-NAVIGATER.

* Healthy controls didn't get tissue NGS testing.

Supplementary Table 5: Ct values of clinical samples, and Horizon standard cfDNA with 1%, 0.1%, 0.01%, and 0% MAF.

Ct values of clinical samples are an average of a duplicate test.

Sample ID	XNA-PCR only		Cas9-DASH XNA-PCR		Once-NAVIGATER XNA-PCR		Twice-NAVIGATER XNA-PCR	
	Ct value	Result	Ct value	Result	Ct value	Result	Ct value	Result
1	35.0	-	38.7	-	38.9	-	39.7	-
2	35.1	-	38.4	-	39.9	-	39.4	-
3	30.4	+	33.7	+	32.6	+	29.7	+
4	34.9	-	38.5	-	38.1	-	38.0	-
5	34.4	-	38.1	-	38.2	-	34.3	+
6	35.0	-	38.4	-	38.4	-	38.8	-
7	34.4	-	33.0	+	32.9	+	30.2	+
8	35.5	-	39.5	-	38.8	-	39.6	-
9	35.0	-	38.5	-	36.3	+	33.9	+
10	35.1	-	39.9	-	39.8	-	39.6	-
11	33.5	Inconclusive*	37.9	-	33.8	+	31.8	+
12	34.9	-	38.3	-	38.0	-	34.8	+
13	34.8	-	39.0	-	39.2	-	39.3	-
14	35.8	-	39.2	-	39.5	-	39.1	-
15	35.8	-	39.5	-	39.6	-	39.6	-
16	35.4	-	39.5	-	39.7	-	39.5	-
17	34.9	-	38.1	-	34.1	+	32.2	+
18	35.7	-	39.9	-	39.7	-	39.7	-
19	34.9	-	38.7	-	38.0	-	39.1	-
20	34.8	-	35.9	+	35.7	+	33.4	+
21	35.2	-	38.6	-	38.3	-	35.3	+
22	35.9	-	39.6	-	39.4	-	39.9	-
1%	30.6	+	33.4	+	32.5	+	30.1	+
0.1%	32.8	+	35.3	+	35.1	+	33.8	+
0.01%	34.1	-	36.5	+	36.2	+	35.1	+
Cutoff (0%)**	33.8 =34.7 - 3x0.3		37.5 =39 - 3x0.5		37.4 =38.9 - 3x0.5		37.2 =39 - 3x0.6	

*" Inconclusive" implies that a mutation was detected once in a duplicate test.

** Cutoff = Average Ct- 3SD (N=5)

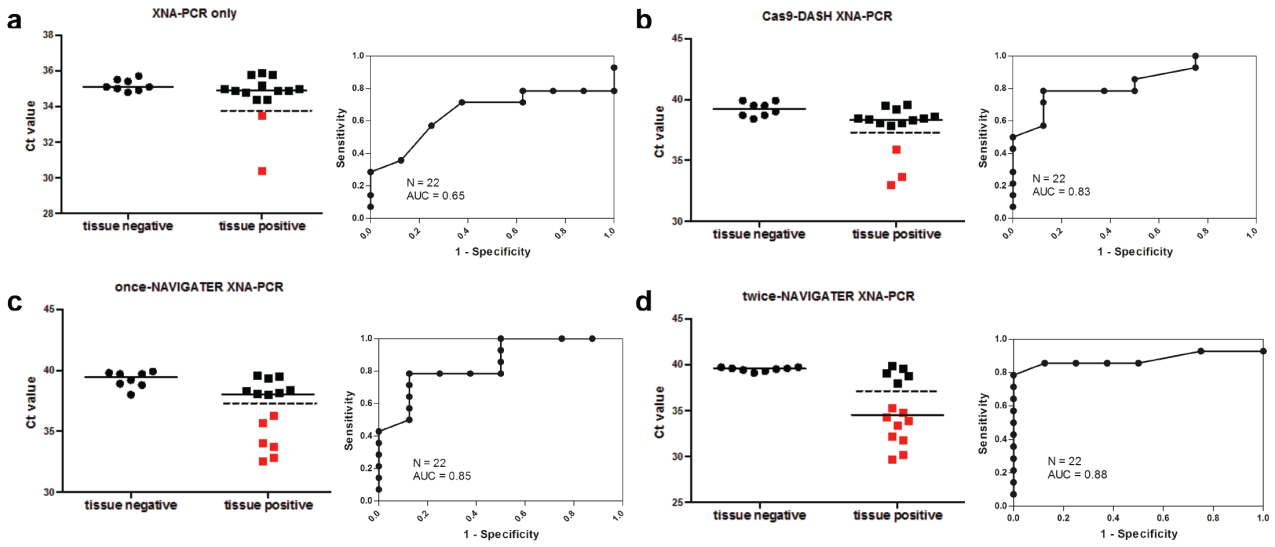

Supplementary Figure 24: Ct values of the 22 tested patient and control samples (left) and ROC curves (right) for (**a**) XNA-PCR only; (**b**) cas9-DASH XNA-PCR; (**c**) once-NAVIGATER XNA-PCR; and (**d**) twice-NAVIGATER XNA-PCR. Solid horizontal lines indicate median values. Dashed horizontal lines indicate cutoff Ct values (Supplementary Table 5).

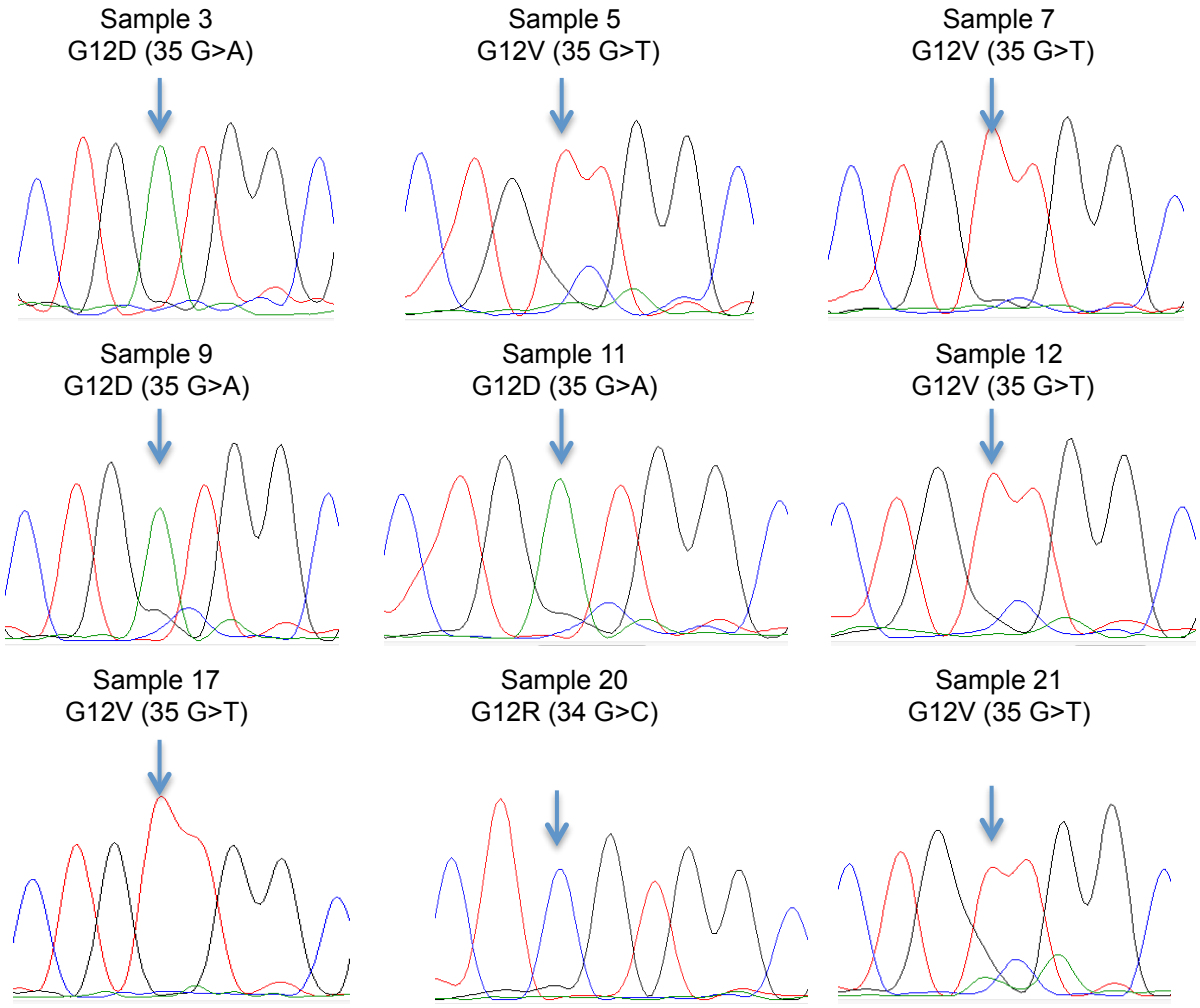

Supplementary Figure 25: Sanger sequencing verification of twice-NAVIGATER XNA-PCR positive samples. Each detected sequence featured a *KRAS* G12 mutation identical to tissue genotype as detected by NGS.

Supplementary Section 9: *Tt*Ago Purification

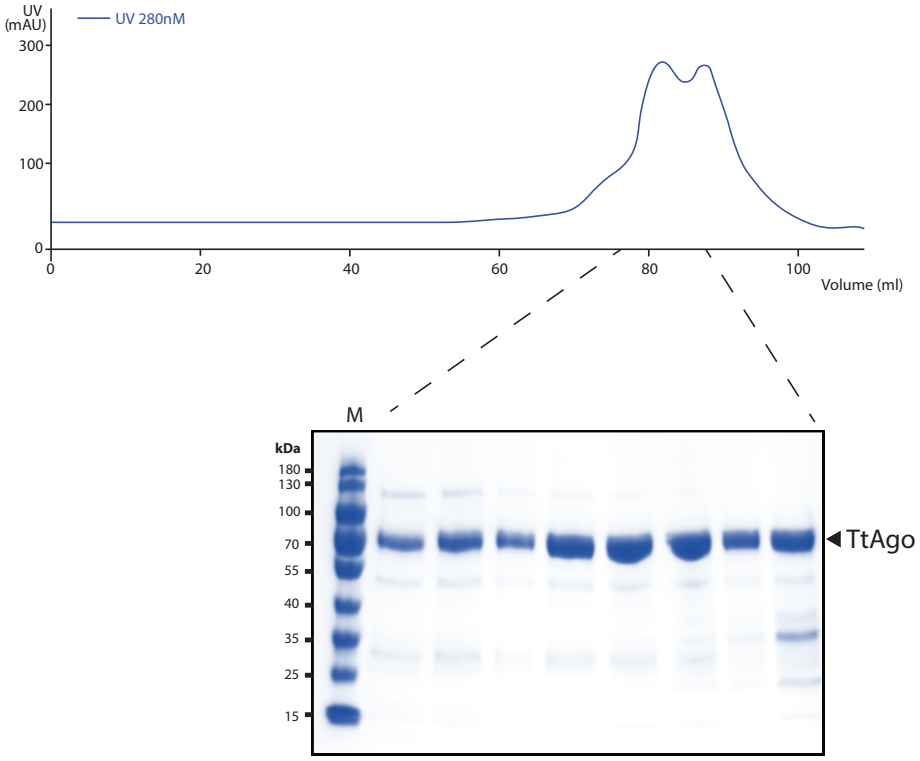

Supplementary Figure 26: Chromatopherogram of purified *Tt*Ago.

Supplementary Section 10: *Tt*Ago deactivation

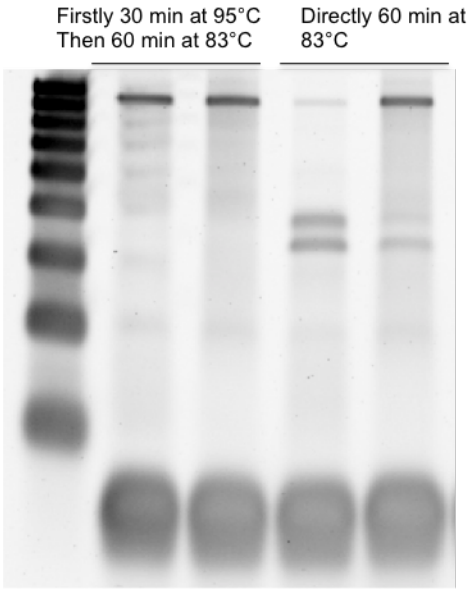

Supplementary Figure 27: *Tt*Ago enzyme is deactivated by incubation at 95°C. The electropherogram shows that an enzyme active at (83^{o}C, control) losses activity after incubation at 95^{o}C for 30 min.

Supplementary References

1. Tatsumi, K., Mitani, Y., Watanabe, J., Takakura, H., Hoshit, K., Kawai, Y., Kikuchi, T., Kogo, Y., Oguchi-Katayama, A., Tomaru, Y. *et al.* (2008) Rapid Screening Assay for KRAS Mutations by the Modified Smart Amplification Process. *Journal of Molecular Diagnostics*, **10**, 520-526.
2. Song, J.Z., Pandian, V., Mauk, M.G., Bau, H.H., Cherry, S., Tisi, L.C. and Liu, C.C. (2018) Smartphone-Based Mobile Detection Platform for Molecular Diagnostics and Spatiotemporal Disease Mapping. *Anal Chem*, **90**, 4823-4831.
3. Swarts, D.C., Jore, M.M., Westra, E.R., Zhu, Y.F., Janssen, J.H., Snijders, A.P., Wang, Y.L., Patel, D.J., Berenguer, J., Brouns, S.J.J. *et al.* (2014) DNA-guided DNA interference by a prokaryotic Argonaute. *Nature*, **507**, 258-+.
4. Sheng, G., Zhao, H.T., Wang, J.Y., Rao, Y., Tian, W.W., Swarts, D.C., van der Oost, J., Patel, D.J. and Wang, Y.L. (2014) Structure-based cleavage mechanism of Thermus thermophilus Argonaute DNA guide strand-mediated DNA target cleavage. *P Natl Acad Sci USA*, **111**, 652-657.
5. Wang, Y.L., Sheng, G., Juranek, S., Tuschl, T. and Patel, D.J. (2008) Structure of the guide-strand-containing argonaute silencing complex. *Nature*, **456**, 209-U234.
6. Wang, Y.L., Juranek, S., Li, H.T., Sheng, G., Wardle, G.S., Tuschl, T. and Patel, D.J. (2009) Nucleation, propagation and cleavage of target RNAs in Ago silencing complexes. *Nature*, **461**, 754-U753.
7. Adamczak, B., Kogut, M. and Czub, J. (2018) Effect of osmolytes on the thermal stability of proteins: replica exchange simulations of Trp-cage in urea and betaine solutions. *Phys Chem Chem Phys*, **20**, 11174-11182.
8. Henke, W., Herdel, K., Jung, K., Schnorr, D. and Loening, S.A. (1997) Betaine improves the PCR amplification of GC-rich DNA sequences. *Nucleic Acids Research*, **25**, 3957-3958.
9. Su, J., Zhong, W.Z., Zhang, X.C., Huang, Y., Yan, H.H., Yang, J.J., Dong, Z.Y., Xie, Z., Zhou, Q., Huang, X.S. *et al.* (2017) Molecular characteristics and clinical outcomes of EGFR exon 19 indel subtypes to EGFR TKIs in NSCLC patients. *Oncotarget*, **8**, 111246-111257.
10. Taly, V., Pekin, D., Benhaim, L., Kotsopoulos, S.K., Le Corre, D., Li, X.Y., Atochin, I., Link, D.R., Griffiths, A.D., Pallier, K. *et al.* (2013) Multiplex Picodroplet Digital PCR to Detect KRAS Mutations in Circulating DNA from the Plasma of Colorectal Cancer Patients. *Clin Chem*, **59**, 1722-1731.
11. Itonaga, M., Matsuzaki, I., Warigaya, K., Tamura, T., Shimizu, Y., Fujimoto, M., Kojima, F., Ichinose, M. and Murata, S. (2016) Novel Methodology for Rapid Detection of KRAS Mutation Using PNA-LNA Mediated Loop-Mediated Isothermal Amplification. *Plos One*, **11**.
12. Gu, W., Crawford, E.D., O'Donovan, B.D., Wilson, M.R., Chow, E.D., Retallack, H. and DeRisi, J.L. (2016) Depletion of Abundant Sequences by Hybridization (DASH): using Cas9 to remove unwanted high-abundance species in sequencing libraries and molecular counting applications. *Genome Biol*, **17**.
13. http://diacarta.com.

Supplementary Note 1
The sequences of guides and synthetic targets

KRAS G12D/V/C guide screening

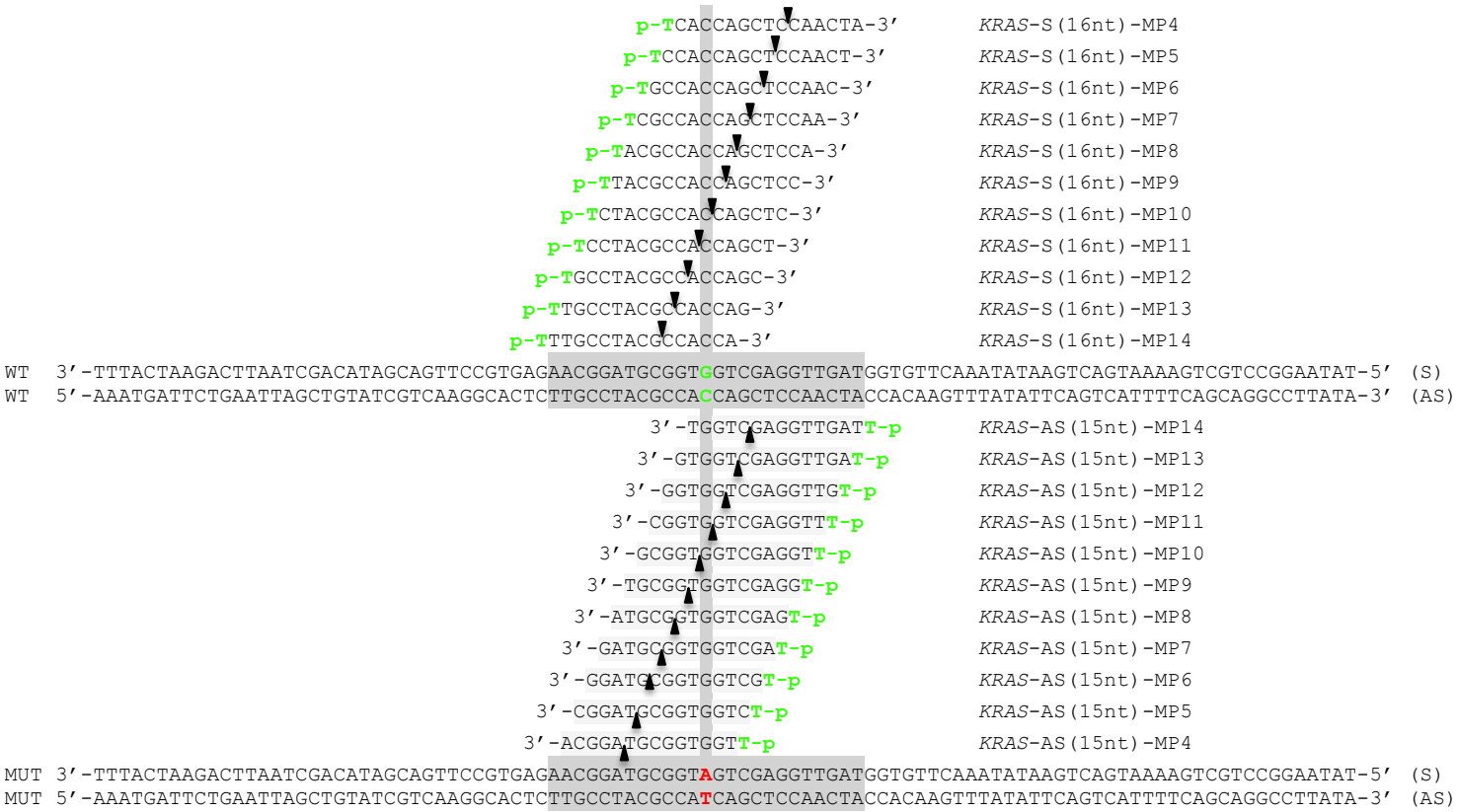

EGFR L858R (2573 T>G) guide screening

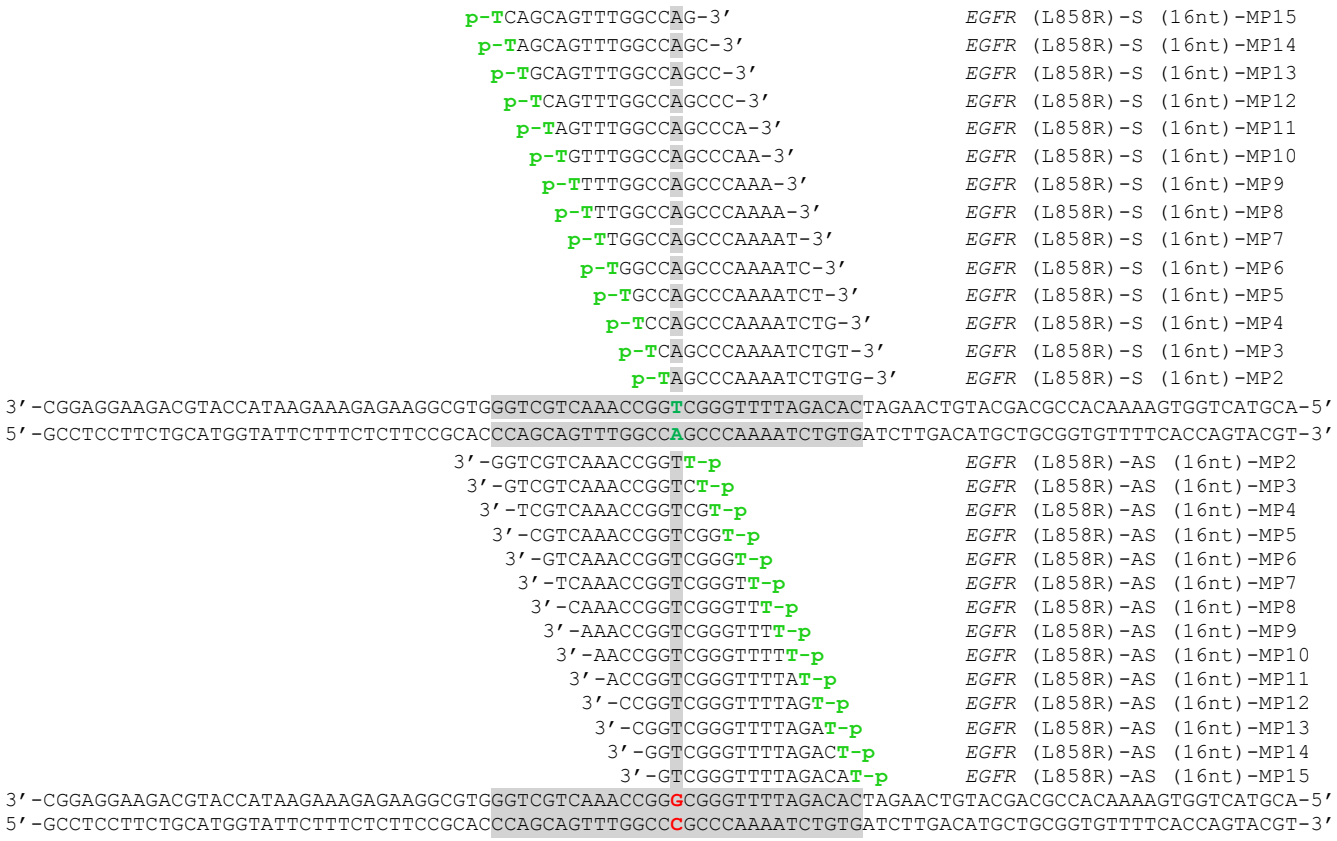

EGFR T790M (2369 C>T) guide screening

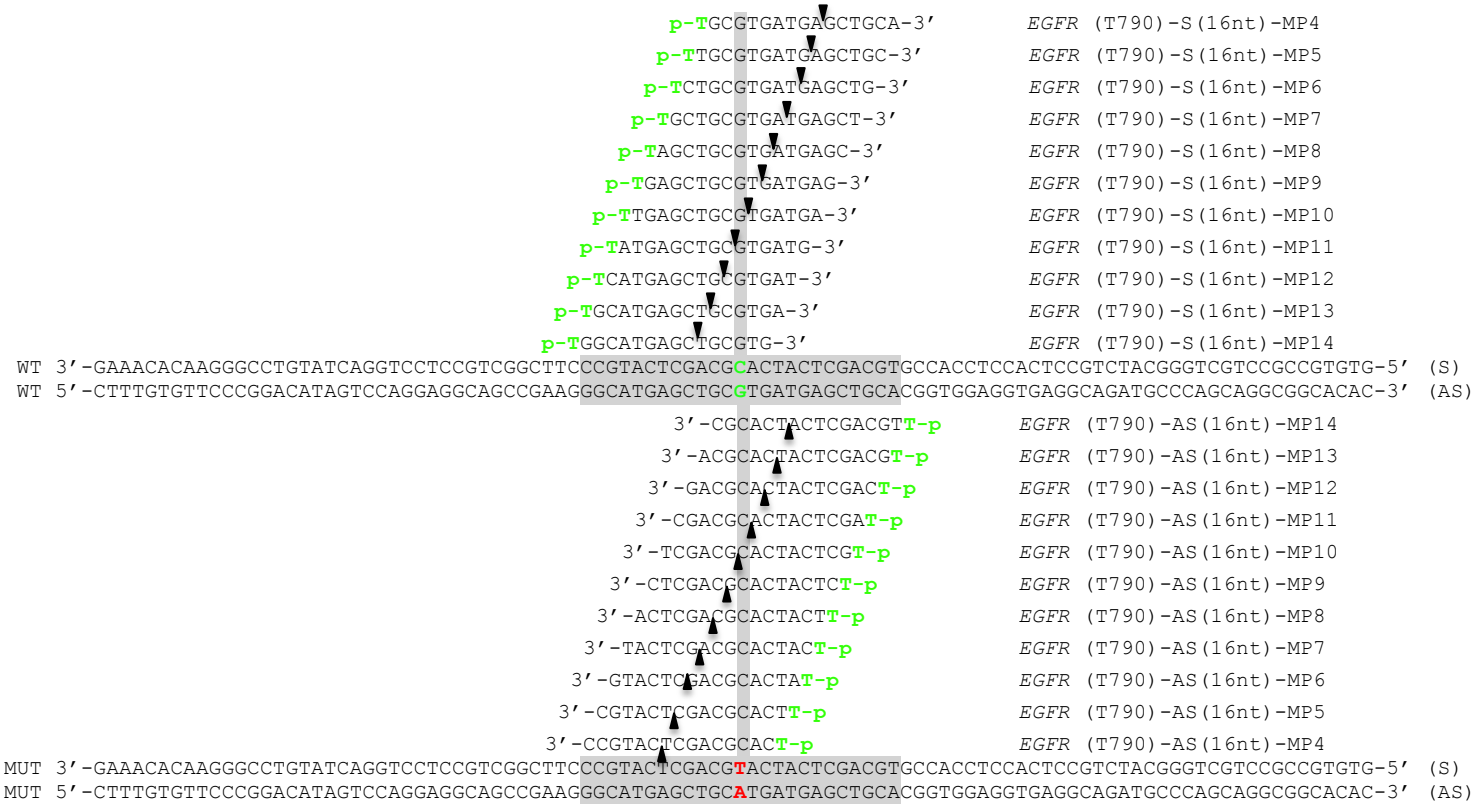

BRAF V600E (1799 T>A) guide screening

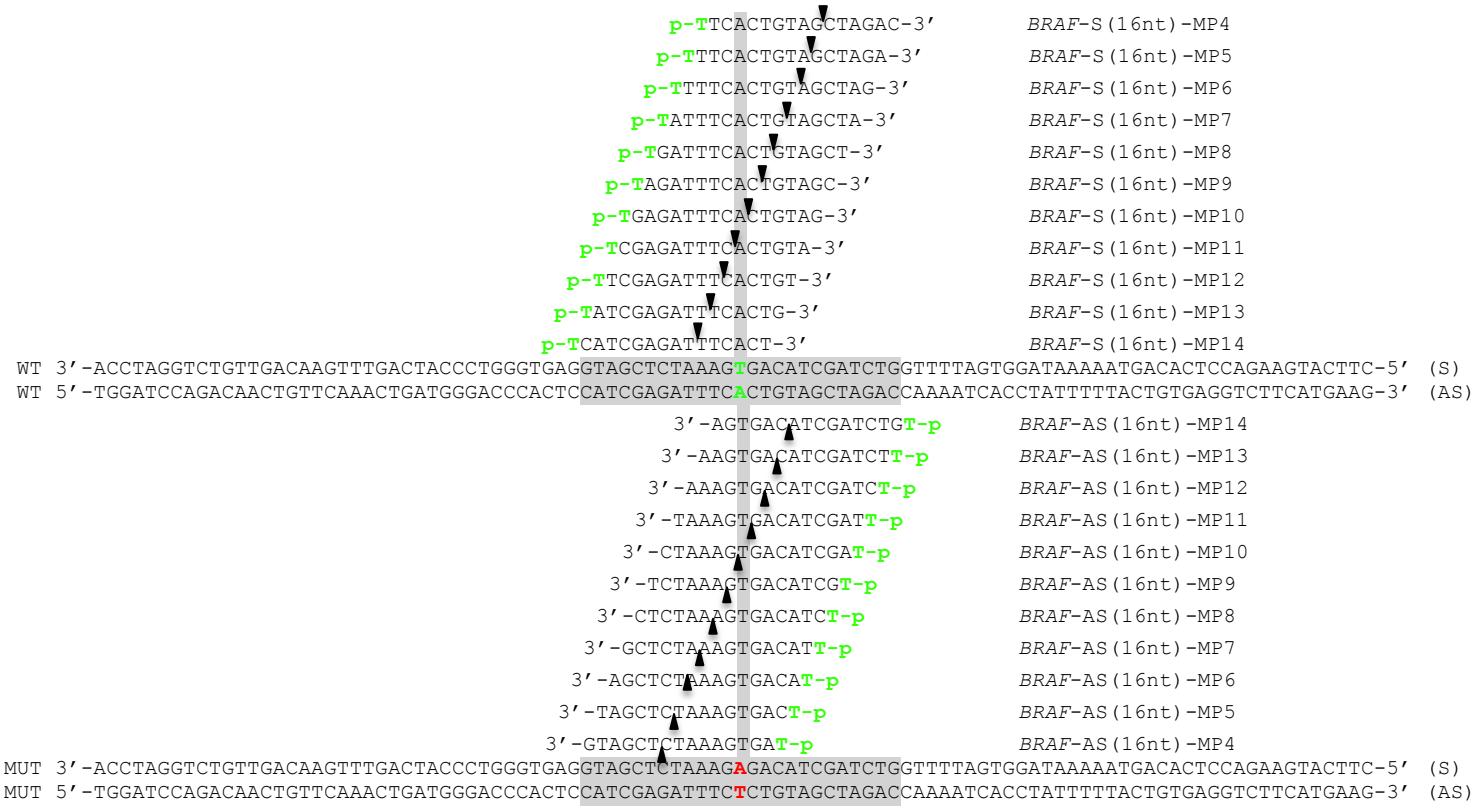

EGFR deletion mutation guide screening

EGFR deletion (Ed) name	Frequency of EGFR exon19 deletion subtypes	Amino acid change	Base pair change	Length (bp)
Ed1	**45%**	p.E746_ A750del(1)	c.2235_2249del15	65
Ed2	**19.6%**	p.E746_ A750del(2)	c.2236_2250del15	65
Ed3	**8.4%**	p.L747_ P753>S	c.2240_2257del18	62
Ed4	**4.3%**	p.L747_ T751del	c.2240_2254del15	65
Ed5	**3.4%**	p.L747_ A750>P	c.2239_2250>cca	71
Ed6	**3.2%**	p.E746_ S752>V(2)	c.2237_2257>ttc	62
Ed7	**1.6%**	p.E746_ S752>V	c.2237_2255>t	62
Ed8	**1.4%**	p.L747_ S752del	c.2239_2256del18	62

```
EGFR deletion mutation-S-guide                    3'-GTTCCTTAATTCTCTT-p
S WT (80bp):       5'-GGTGAGAAAGTTAAAATTCCCGTCGCTATCAAGGAATTAAGAGAAGCAACATCTCCGAAAGCCAACAAGGAAATCCTCGA-3'
S 2235_2249del15:  5'-GGTGAGAAAGTTAAAATTCCCGTCGCTATCAA---------------AACATCTCCGAAAGCCAACAAGGAAATCCTCGA-3'
S 2236_2250del15:  5'-GGTGAGAAAGTTAAAATTCCCGTCGCTATCAAG--------------ACATCTCCGAAAGCCAACAAGGAAATCCTCGA-3'
S 2240_2257del18:  5'-GGTGAGAAAGTTAAAATTCCCGTCGCTATCAAGGAAT-----------------CGAAAGCCAACAAGGAAATCCTCGA-3'
S 2240_2254del15:  5'-GGTGAGAAAGTTAAAATTCCCGTCGCTATCAAGGAAT---------------CTCCGAAAGCCAACAAGGAAATCCTCGA-3'
S 2239_2250>cca:   5'-GGTGAGAAAGTTAAAATTCCCGTCGCTATCAAGGAA----CCA-----ACATCTCCGAAAGCCAACAAGGAAATCCTCGA-3'
S 2237_2257>ttc:   5'-GGTGAGAAAGTTAAAATTCCCGTCGCTATCAAGG------TTC------------CGAAAGCCAACAAGGAAATCCTCGA-3'
S 2237_2255>t:     5'-GGTGAGAAAGTTAAAATTCCCGTCGCTATCAAGG-------T-----------TCCGAAAGCCAACAAGGAAATCCTCGA-3'
S 2239_2256del18:  5'-GGTGAGAAAGTTAAAATTCCCGTCGCTATCAAGGAA-----------------CCGAAAGCCAACAAGGAAATCCTCGA-3'

EGFR deletion mutation-AS-guide                          p-TAAGAGAAGCAACATC-3'
AS WT (80bp):      3'-CCACTCTTTCAATTTTAAGGGCAGCGATAGTTCCTTAATTCTCTTCGTTGTAGAGGCTTTCGGTTGTTCCTTTAGGAGCT-5'
AS 2235_2249del15: 3'-CCACTCTTTCAATTTTAAGGGCAGCGATAGTT---------------TTGTAGAGGCTTTCGGTTGTTCCTTTAGGAGCT-5'
AS 2236_2250del15: 3'-CCACTCTTTCAATTTTAAGGGCAGCGATAGTTC---------------TGTAGAGGCTTTCGGTTGTTCCTTTAGGAGCT-5'
AS 2240_2257del18: 3'-CCACTCTTTCAATTTTAAGGGCAGCGATAGTTCCTTA-----------------GCTTTCGGTTGTTCCTTTAGGAGCT-5'
AS 2240_2254del15: 3'-CCACTCTTTCAATTTTAAGGGCAGCGATAGTTCCTTA---------------GAGGCTTTCGGTTGTTCCTTTAGGAGCT-5'
AS 2239_2250>cca:  3'-CCACTCTTTCAATTTTAAGGGCAGCGATAGTTCCTT----GGT-----TGTAGAGGCTTTCGGTTGTTCCTTTAGGAGCT-5'
AS 2237_2257>ttc:  3'-CCACTCTTTCAATTTTAAGGGCAGCGATAGTTCC------AAG------------GCTTTCGGTTGTTCCTTTAGGAGCT-5'
AS 2237_2255>t:    3'-CCACTCTTTCAATTTTAAGGGCAGCGATAGTTCC-------A-----------AGGCTTTCGGTTGTTCCTTTAGGAGCT-5'
AS 2239_2256del18: 3'-CCACTCTTTCAATTTTAAGGGCAGCGATAGTTCCTT-----------------GGCTTTCGGTTGTTCCTTTAGGAGCT-5'
```

Longer guides (18/19nt)--*KRAS* G12D/V/C guide screening

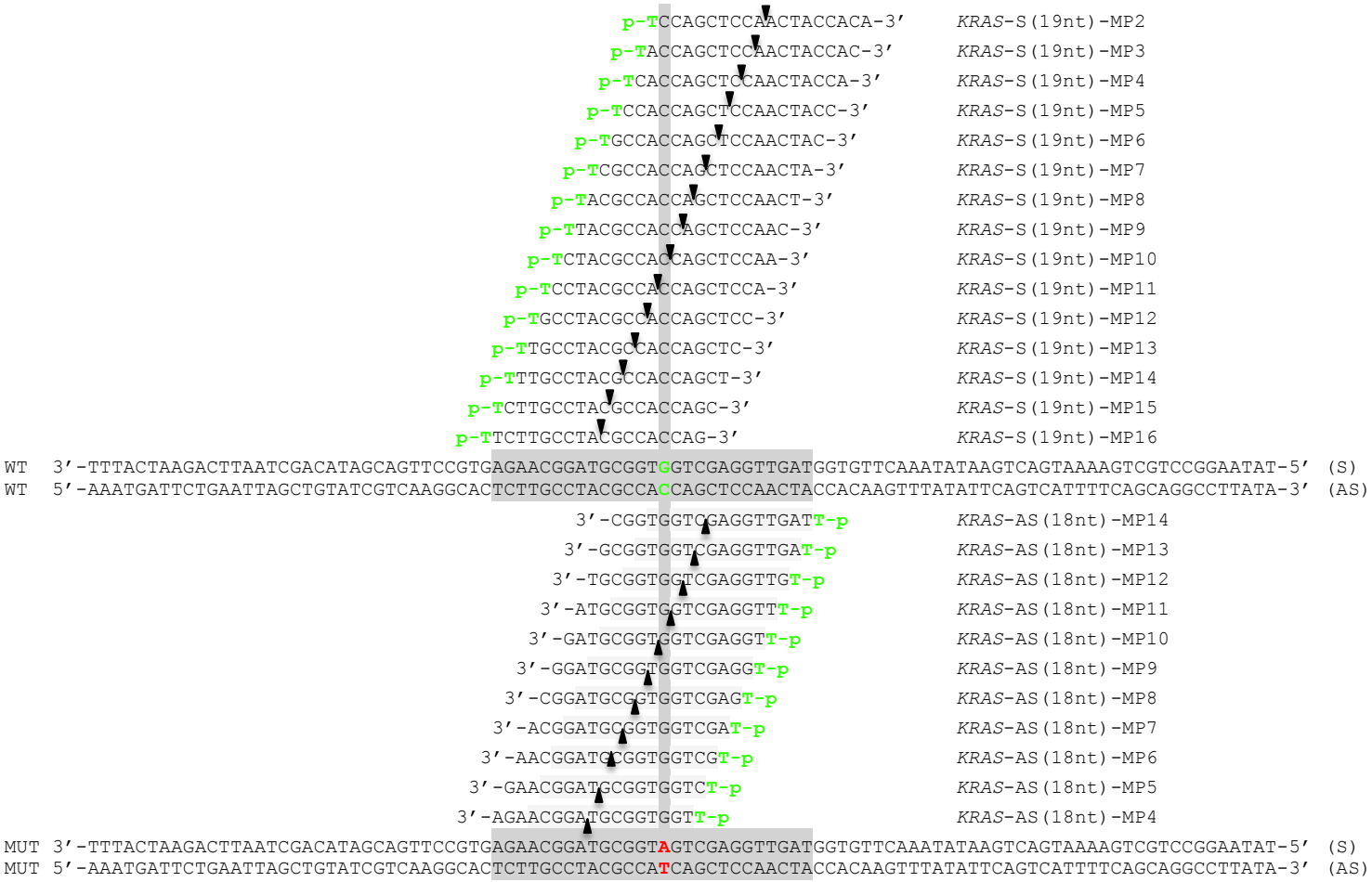

The sequences of synthetic targets with various GC content and guides

GC-68.9%

S:
TCC GCT CGG GGC GGC ACC GGG AAC CTG AGC CGT GCG AAC GCA TAC GAC TGA TCT GAG CAC TCC TGT CTC CGG CCC AAG CCA GGG GTG CGG

AS:
CCG CAC CCC TGG CTT GGG CCG GAG ACA GGA GTG CTC AGA TCA GTC GTA TGC GTT CGC ACG GCT CAG GTT CCC GGT GCC GCC CCG AGC GGA

GC-50%

S:
TCG ACT GCT CGG TCG CTT TTC GCA CTC CGC GAA AGT TCG TAC ATA CGA CTG ATC TGA GCA CTA AGC CTA TGC TGA TAT ATG GAT CCA GAC

AS:
GTC TGG ATC CAT ATA TCA GCA TAG GCT TAG TGC TCA GAT CAG TCG TAT GTA CGA ACT TTC GCG GAG TGC GAA AAG CGA CCG AGC AGT CGA

GC-31.1%

S:
TAA TGA CTT AAC ACG TTA AGA ACA TGA AAT TGA TTC TTT CGC ATA CGA CTG ATC TGA GCA CTA GAA TGT TAT ATG AAG TAT GAA TAT AAC

AS:
GTT ATA TTC ATA CTT CAT ATA ACA TTC TAG TGC TCA GAT CAG TCG TAT GCG AAA GAA TCA ATT TCA TGT TCT TAA CGT GTT AAG TCA TTA

Guide:

S: AGT GCT CAG ATC AGT C

AS: CAT ACG ACT GAT CTG A